Fuzzy Adaptive Zero-Error-Constrained Tracking Control for HFVs in the Presence of Multiple Unknown Control Directions

Lv, Maolong; De Schutter, Bart; Wang, Ying; Shen, Di

Important note
To cite this publication, please use the final published version (if applicable).
Please check the document version above.

Fuzzy Adaptive Zero-Error-Constrained Tracking Control for HFVs in the Presence of Multiple Unknown Control Directions

Maolong Lv[ID], Bart De Schutter, *Fellow, IEEE*, Ying Wang, and Di Shen

Abstract—This article attempts to realize zero-error constrained tracking for hypersonic flight vehicles (HFVs) subject to unknown control directions and asymmetric flight state constraints. The main challenges of reaching such goals consist in that addressing multiple unknown control directions requires novel conditional inequalities encompassing the summation of multiple Nussbaum integral terms, and in that the summation of conditional inequality may be bounded even when each term approaches infinity individually, but with opposite signs. To handle this challenge, novel Nussbaum functions that are designed in such a way that their signs keep the same on some periods of time are incorporated into the control design, which not only ensures the boundedness of multiple Nussbaum integral terms but preserves that velocity and altitude tracking errors eventually converge to zero. Fuzzy-logic systems (FLSs) are exploited to approximate model uncertainties. Asymmetric integral barrier Lyapunov functions (IBLFs) are adopted to handle the fact that the operating regions of flight state variables are asymmetric in practice, while ensuring the validity of fuzzy-logic approximators. Comparative simulations validate the effectiveness of our proposed methodology in guaranteeing convergence, smoothness, constraints satisfaction, and in handling unknown control directions.

Index Terms—Flight state constraints, hypersonic flight vehicles, unknown control directions, zero-error tracking.

I. INTRODUCTION

HYPERSONIC flight vehicles have been attracting a tremendous attention due to its significant civilian and military value [1]–[6]. Different from traditional flight vehicles, HFVs adopt the distinguishing airframe/scramjet integration and wave-rider configuration, which unavoidably leads to strong couplings between propulsive and aerodynamic forces [7]–[11]. The research on flight control design for HFVs in past decades comprises observer-based control [12], [13], sliding-mode control [14], [15], intelligent control [16]–[18],

and so on. However, it is worth underlining that all above-mentioned approaches neglect crucial aspects of HFVs, such as multiple unknown control directions and zero-error tracking. The importance of those perspectives is explained hereafter.

Control direction, which is the so-called sign of control gain function, is typically assumed known *a priori* to feedback control design [19]. In case the control direction of a control system is unknown *a priori*, designing a controller becomes challenging since a control force with incorrect control direction might steer the system away from the desired behavior or even causes instability. During the hypersonic flight, the problem of unknown control directions arises because: on the one hand, it has been shown in simulation data provided by NASA Langley Research Center [20] that the aerodynamic coefficients vary with respect to flight conditions. At the same time, the rapid-varying aerodynamic coefficients are practically difficult to accurately measure due to the high speed and agile manoeuvring, leading to unknown control directions [21]. On the other hand, massive applications of telex components inevitably bring the reverse fault when the control signal is transmitted from flight control computer to aerodynamic control surfaces, such as canard and elevator, posing opposite control directions [20], [21]. Nussbaum function originally proposed in [22] has been extensively adopted in the available literature [23]–[27] to handle an unknown control direction and its working mechanism is to alternatively (periodically in most scenarios) change the sign of control force in an adaptive design. A fundamental tool is the technical lemma that guarantees the boundedness of a Lyapunov-like energy function when its derivative along a system is upper bounded by a Nussbaum function-based fashion [28]. It has to be pointed out that [29] and [30] have shown that the summation of multiple Nussbaum integral terms may be bounded even when each term approaches infinity individually, but with opposite signs since their effects might counteract each other. Despite some works [31], [32] proposed new Nussbaum gain technical lemmas, some restrictive requirements, including assuming unknown but identical control directions [31] and mixed unknown control directions (some being known, some being unknown) via a piecewise Nussbaum function that exploits a priori knowledge of the known control directions [32], need to be satisfied. This, however, is hardly applied to HFVs where control directions are usually unpredictable and vary along with flight state variables [20], [21].

On account of the physical constraints that characterize hypersonic flight and operability of scramjet engines, the flight state variables have upper and lower magnitude constraints in practice, and the violation of these constraints may deteriorate system performance and even endanger flight safety [33]–[35]. The barrier Lyapunov function (BLF) first [36]–[38] and integral Lyapunov function later [39]–[42] are employed to guarantee the nonviolation of state constraints, while ensuring closed-loop stability. Although [37] took state constraints into consideration, it can solely achieve bounded tracking errors, that is, tracking errors converge to a residual set rather than zero. Given the high speed and super maneuver of HFVs, accurate tracking is of paramount importance in executing various flight missions and a new flight control design going beyond the available approaches must be sought. The discussions above motivates this study whose innovations are listed as follows.

1) Compared with the bounded tracking results, this article achieves zero-error tracking for the longitudinal dynamics, while at the same time considering multiple unknown control directions and flight state constraints.

2) To handle multiple unknown control directions, novel Nussbaum functions whose sign keeps the same on some periods of time are proposed such that the effects of multiple Nussbaum integral terms do not cancel each other in the summation, which paves the way to obtain the boundedness of multiple Nussbaum integral terms during the stability analysis.

3) Integral barrier Lyapunov functions are exploited to confine flight state variables within some user-defined compact sets all the time provided their initial values remain therein. This property also guarantees the validity of fuzzy-logic approximators.

The remainder of this article is organized as follows. The considered problem is formulated in Section II. Sections III and IV present the control design and stability analysis, respectively. Simulation results are given in Section V, and Section VI draws the conclusion.

II. VEHICLE MODEL AND PROBLEM FORMULATION

A. Hypersonic Flight Vehicle Dynamics

The HFVs model adopted in this article is originally developed by Bolender and Doman [9]. The motion equations, derived from Lagrange's equations, involve the flexible effects by modeling the fuselage as a free beam. The mathematical description of the longitudinal dynamics is as follows:

$$\dot{V} = \frac{T \cos \alpha - D}{m} - g \sin \gamma \tag{1}$$

$$\dot{h} = V \sin \gamma, \tag{2}$$

$$\dot{\gamma} = \frac{L + T \sin \alpha}{mV} - \frac{g \cos \gamma}{V} \tag{3}$$

$$\dot{\alpha} = Q - \frac{L + T \sin \alpha}{mV} + \frac{g \cos \gamma}{V} \tag{4}$$

$$\dot{Q} = \frac{M}{I_{yy}} \tag{5}$$

$$\ddot{\eta}_i = -2\zeta_i \omega_i \dot{\eta}_i - \omega_i^2 \eta_i + N_i, \quad i = 1, \ldots, n \tag{6}$$

where the lift L, drag D, pitching moment M, thrust T, and generalized elastic forces N_i are given as

$$L = \bar{q} S C_L(\alpha, \delta_e, \delta_c, \boldsymbol{\eta}) \tag{7}$$

$$D = \bar{q} S C_D(\alpha, \delta_e, \delta_c, \boldsymbol{\eta}) \tag{8}$$

$$M = z_T T + \bar{q} S \bar{c} C_M(\alpha, \delta_e, \delta_c, \boldsymbol{\eta}) \tag{9}$$

$$T = \bar{q} S \big[C_{T,\Phi}(\alpha) \Phi + C_T(\alpha) + \boldsymbol{C}_T^{\boldsymbol{\eta}} \boldsymbol{\eta} \big] \tag{10}$$

$$N_i = \bar{q} S \big[N_i^{\alpha^2} \alpha^2 + N_i^{\alpha} \alpha + N_i^{\delta_e} \delta_e + N_i^{\delta_c} \delta_c $$
$$+ N_i^0 + \boldsymbol{N}_i^{\boldsymbol{\eta}} \boldsymbol{\eta} \big], \quad i = 1, \ldots, n. \tag{11}$$

The considered model (1)–(11) contains five rigid-body states, that is: 1) velocity V; 2) altitude h; 3) flight path angle (FPA) γ; 4) angle of attack (AOA) α; and 5) pitch rate Q, and three control inputs, that is: 1) the fuel equivalence ratio Φ; 2) deflection of elevator δ_e; and 3) deflection of canard δ_c. $\boldsymbol{\eta} = [\eta_1, \dot{\eta}_1, \ldots, \eta_n, \dot{\eta}_n]^T$, $n \in \mathbb{N}^+$ are the flexible states with η_i being the amplitude of the ith bending mode. m, I_{yy}, g, ζ_i, ω_i, $\bar{q}$, S, z_T, and $\bar{c}$ represent the vehicle mass, moment of inertia, gravitational acceleration, damping ratio, flexible mode frequency, dynamic press, reference area, thrust moment arm, and reference length, respectively. The coefficients obtained from fitting the curves are given as follows:

$$C_M(\cdot) = C_M^{\alpha^2} \alpha^2 + C_M^{\alpha} \alpha + C_M^{\delta_e} \delta_e + C_M^{\delta_c} \delta_c + C_M^0 + \boldsymbol{C}_M^{\boldsymbol{\eta}} \boldsymbol{\eta}$$
$$C_L(\cdot) = C_L^{\alpha} \alpha + C_L^{\delta_e} \delta_e + C_L^{\delta_c} \delta_c + C_L^0 + \boldsymbol{C}_L^{\boldsymbol{\eta}} \boldsymbol{\eta}$$
$$C_D(\cdot) = C_D^{\alpha^2} \alpha^2 + C_D^{\alpha} \alpha + C_D^{\delta_e^2} \delta_e^2 + C_D^{\delta_e} \delta_e$$
$$\quad + C_D^{\delta_c^2} \delta_c^2 + C_D^{\delta_c} \delta_c + C_D^0 + \boldsymbol{C}_D^{\boldsymbol{\eta}} \boldsymbol{\eta}$$
$$C_{T,\Phi}(\cdot) = C_{T,\Phi}^{\alpha^3} \alpha^3 + C_{T,\Phi}^{\alpha^2} \alpha^2 + C_{T,\Phi}^{\alpha} \alpha + C_{T,\Phi}^0$$
$$C_T(\cdot) = C_T^{\alpha^3} \alpha^3 + C_T^{\alpha^2} \alpha^2 + C_T^{\alpha} \alpha + C_T^0$$
$$\boldsymbol{C}_j^{\boldsymbol{\eta}} = \big[C_j^{\eta_1}, 0, \ldots, C_j^{\eta_n}, 0 \big], \quad j = T, M, L, D$$
$$\boldsymbol{N}_i^{\boldsymbol{\eta}} = \big[N_i^{\eta_1}, 0, \ldots, N_i^{\eta_n}, 0 \big], \quad i = 1, \ldots, n. \tag{12}$$

To cancel the lift-elevator coupling, δ_c is set to be ganged with δ_e, that is, $\delta_c = k_{e,c} \delta_e$ with $k_{e,c} = -C_L^{\delta_e}/C_L^{\delta_c}$. Thereby, the control inputs of HFVs become Φ and δ_e. It is worth mentioning that the rigid-body states in (1)–(5) must operate in constrained regions that are not symmetric. A typical operating region characterizing hypersonic flight and operability of scramjet engines can be the hypercube [7]

$$\Omega_0 = \{85000 \leq h \leq 135000[\text{ft}], 7500 \leq V \leq 11500[\text{ft/s}]$$
$$-5 \leq \theta \leq 10[\text{deg}], -10 \leq Q \leq 10[\text{deg/s}], -5 \leq \gamma \leq 7[\text{deg}]\}.$$

For flight safety and reliability, the smooth reference trajectories V_r and h_r are confined to a subset $\Omega_r \subset \Omega_0$. This study aims at developing a Nussbaum gain adaptive tracking control method satisfying that: 1) h and V track the reference signals h_r and V_r asymptotically, namely, $h - h_r \to 0$ and $V - V_r \to 0$ as $t \to \infty$; 2) the asymmetric flight state constraints are never transgressed; and 3) all closed-loop signals remain bounded.

Refer to Fig. 1 for a sketch of force map and airframe. The elevator angular deflection δ_e primarily affects the AOA α (hence, altitude h), whereas the fuel equivalence ratio Φ primarily affects the thrust T (hence, velocity V). Based on
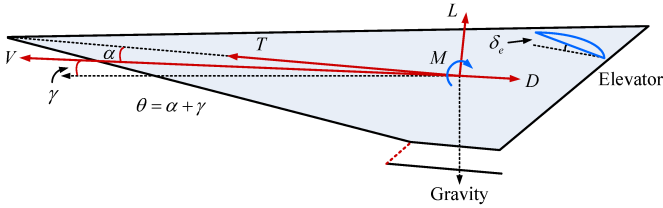
Fig. 1. Schematic and force map of HFVs.

Fig. 2. Block diagram of the reverse fault form.

these physical considerations, related literature has proposed a model decomposition amenable for control design [16]–[18].

B. Model Decomposition

Since the flexible states $\boldsymbol{\eta}$ are hard to obtain in practice, we treat the flexible dynamics as unknown disturbances in our design stage, while their effects have been discussed in [13]. Taking aerodynamic parameter uncertainties and external disturbances into account, the velocity dynamics (1) can be rewritten as [16]–[18]

$$\dot{V} = \boldsymbol{\zeta}_V^T(\boldsymbol{f}_V + \boldsymbol{g}_V \Phi) + d_V \qquad (13)$$

where $\boldsymbol{\zeta}_V = (S/m)[C_{T,\Phi}^{\alpha^3}, C_{T,\Phi}^{\alpha^2}, C_{T,\Phi}^{\alpha}, C_{T,\Phi}^{0}, C_T^{\alpha^3}, C_T^{\alpha^2}, C_T^{\alpha}, C_T^{0},$
$C_D^{\alpha^2}, C_D^{\alpha}, (C_D^{\delta_e^2} + k_{e,c}^2 C_D^{\delta_c^2}), (C_D^{\delta_e} + k_{e,c} C_D^{\delta_c}), C_D^{0}, (m/S)]^T$, $\boldsymbol{g}_V = \bar{q} \cos\alpha[\alpha^3, \alpha^2, \alpha, 1, \mathbf{0}^{1\times 10}]^T$, $\boldsymbol{f}_V = \bar{q}[\mathbf{0}^{1\times 4}, \alpha^3 \cos\alpha, \alpha^2 \cos\alpha,$
$\alpha \cos\alpha, \cos\alpha, \quad -\alpha^2, -\alpha, \quad -\delta_e^2, -\delta_e, \quad -1, -(g/\bar{q})\sin\gamma]^T$, and the lumped disturbance $d_V = (\bar{q}S/m)C_T^{\eta}\boldsymbol{\eta}\cos\alpha - (\bar{q}S/m)C_D^{\eta}\boldsymbol{\eta} + \Delta_V$ with Δ_V denoting the perturbations resulting from coefficients uncertainties and external disturbances in the velocity dynamics.

In general, the FPA γ and AOA α are quite small during the cruise phase; here, we take $\sin\gamma \approx \gamma$ in (2) and neglect $T\sin\alpha$ in (3) for simplicity [13], [37]. Therefore, the altitude dynamics (2)–(5) can be rewritten as [16]–[18]

$$\begin{cases} \dot{h} = V\gamma + d_h \\ \dot{\gamma} = \boldsymbol{\zeta}_\gamma^T(\boldsymbol{f}_\gamma + \boldsymbol{g}_\gamma \alpha) + d_\gamma \\ \dot{\alpha} = \boldsymbol{\zeta}_\alpha^T(\boldsymbol{f}_\alpha + \boldsymbol{g}_\alpha Q) + d_\alpha \\ \dot{Q} = \boldsymbol{\zeta}_Q^T(\boldsymbol{f}_Q + \boldsymbol{g}_Q \delta_e) + d_Q \end{cases} \qquad (14)$$

where $\boldsymbol{\zeta}_\gamma = [(S/m)C_L^{\alpha}, (S/m)C_L^{0}, 1]^T$, $\boldsymbol{\zeta}_\alpha = [1, (S/m)C_L^{\alpha}, (S/m)C_L^{0}, 1]^T$, $\boldsymbol{\zeta}_Q = (S/I_{yy})[\bar{c}C_M^{\delta_e}, \bar{c}k_{e,c}C_M^{\delta_c}, z_T C_{T,\Phi}^{\alpha^3}, z_T C_{T,\Phi}^{\alpha^2}, \quad z_T C_{T,\Phi}^{\alpha}, z_T C_{T,\Phi}^{0}, \quad z_T C_T^{\alpha^3}, (z_T C_T^{\alpha^2} + \bar{c}C_M^{\alpha^2}), (z_T C_T^{\alpha} + \bar{c}C_M^{\alpha}), (z_T C_T^{0} + \bar{c}C_M^{0})]^T$, $\boldsymbol{g}_\gamma = [(\bar{q}/V), \mathbf{0}^{1\times 2}]^T$, $\boldsymbol{g}_\alpha = [1, \mathbf{0}^{1\times 3}]^T$, $\boldsymbol{g}_Q = [\bar{q}, \bar{q}, \mathbf{0}^{1\times 8}]^T$, $\boldsymbol{f}_\gamma = [0, (\bar{q}/V), -(g/V)\cos\gamma]^T$, $\boldsymbol{f}_\alpha = (\bar{q}/V)[0, -\alpha, -1, (g/\bar{q})\cos\gamma]^T$, $\boldsymbol{f}_Q = \bar{q}[\mathbf{0}^{1\times 2}, \alpha^3\Phi, \alpha^2\Phi, \alpha\Phi, \Phi, \alpha^3, \alpha^2, \alpha, 1]^T$, and the lumped disturbances $d_h = \Delta_h$, $d_\gamma = (\bar{q}S/mV)C_L^{\eta}\boldsymbol{\eta} + \Delta_\gamma$, $d_\alpha = -(\bar{q}S/mV)C_L^{\eta}\boldsymbol{\eta} + \Delta_\alpha$, and $d_Q = (z_T\bar{q}S/I_{yy})C_T^{\eta}\boldsymbol{\eta} + (\bar{q}S\bar{c}/I_{yy})C_M^{\eta}\boldsymbol{\eta} + \Delta_Q$, with $\Delta_h, \Delta_\gamma, \Delta_\alpha$, and Δ_Q representing the perturbations resulting from coefficient uncertainties and external disturbances in the altitude dynamics. Let us define the signs of control gain functions as $s_1 = \text{sgn}(\boldsymbol{\zeta}_V^T\boldsymbol{g}_V)$, $s_2 = \text{sgn}(\boldsymbol{\zeta}_\gamma^T\boldsymbol{g}_\gamma)$, $s_3 = \text{sgn}(\boldsymbol{\zeta}_\alpha^T\boldsymbol{g}_\alpha)$, and $s_4 = \text{sgn}(\boldsymbol{\zeta}_Q^T\boldsymbol{g}_Q)$, and the functions $g_1 = |\boldsymbol{\zeta}_V^T\boldsymbol{g}_V|$, $g_2 = |\boldsymbol{\zeta}_\gamma^T\boldsymbol{g}_\gamma|$, $g_3 = |\boldsymbol{\zeta}_\alpha^T\boldsymbol{g}_\alpha|$, and $g_4 = |\boldsymbol{\zeta}_Q^T\boldsymbol{g}_Q|$.

Assumption 1 [17], [18]: There exist constants $\bar{g}_i > 0$ and $\underline{g}_i > 0$, $i = 1, \ldots, 4$, such that $\underline{g}_i \leq g_i \leq \bar{g}_i$, $i = 1, \ldots, 4$.

Remark 1: Assumption 1 has been widely used in [13], [17], and [18] to guarantee the controllability for dynamics (13) and (14). HFVs do have an uncertain problem with multiple unknown control directions since the control gain functions of velocity and altitude channels are some continuous functions of various aerodynamic coefficients whose values might be varying along with flight environment according to [20]. Besides, reverse fault may occur in telex systems and also poses the issue of unknown control directions when the control signal is transmitted from flight control computer to actuators [21] as shown in Fig. 2.

C. Technical Key Lemmas

The following lemmas will be used for control design and stability analysis in the subsequent sections.

Definition 1 [22]: A continuous even function $\mathcal{N}(\cdot)$ is called Nussbaum-type when it satisfies the following properties:

$$\lim_{\omega\to\infty} \frac{\sup \int_0^\omega \mathcal{N}(\tau)d\tau}{\omega} = +\infty, \quad \lim_{\omega\to\infty} \frac{\inf \int_0^\omega \mathcal{N}(\tau)d\tau}{\omega} = -\infty.$$

For velocity dynamics (13) and altitude dynamics (14), we propose a class of new Nussbaum functions in the form of

$$\mathcal{N}_i(\omega) = \left(\mu(\omega)\sin(2^i\omega) + 2^i\omega\cos(2^i\omega)\right) \times \exp(\omega^2), \quad i = 1, \ldots, 4 \qquad (15)$$

where $\mu(\omega) = 2\omega^2 + 1$.

By direct calculation, one reaches

$$\int_0^\omega \mathcal{N}_i(\tau)d\tau = \sin(2^i\omega)\omega\exp(\omega^2). \qquad (16)$$

Lemma 1: The Nussbaum functions in (15) have the following properties.
1) $\mathcal{N}_i(\omega)$ is a smooth odd function of ω.
2) $\int_0^\omega \mathcal{N}_i(\tau)d\tau$ is an even function of ω.
3) Define $\Theta_i(\omega) = s_i\sin(2^i\omega)$. Then, the frequencies of $\Theta_1(\omega), \ldots, \Theta_4(\omega)$ consist of a geometric progression with the common ratio 2.
4) $|\Theta_i(\omega)| \geq 2^{i-4}|\Theta_4(\omega)|$ for all $\omega \in \mathbb{R}$ and $i = 1, \ldots, 4$.

Proof: The first three properties are obvious from (15) and (16). To show the last one, define

$$M_i(\omega) = |\Theta_i(\omega)| - 2^{i-4}|\Theta_4(\omega)|.$$

Let us first consider the case $\omega \in [0, 2^{-5}\pi]$, where $M_i(\omega) = \sin(2^i\omega) - 2^{i-4}\sin(2^4\omega)$ and $(dM_i(\omega)/d\omega) = 2^i\cos(2^i\omega) - 2^i\cos(2^4\omega) \geq 0$. Hence

$$M_i(\omega) \geq M_i(0) = 0 \quad \forall\omega \in \left[0, 2^{-5}\pi\right].$$

Letting $\omega = 2^{-5}\pi$, and noting that $|\Theta_4(2^{-5}\pi)| = 1$, it follows that:

$$\left|\Theta_i\left(2^{-5}\pi\right)\right| \geq 2^{i-4}\left|\Theta_4\left(2^{-5}\pi\right)\right| = 2^{i-4}.$$

Then, let us consider the case $\omega \in [2^{-5}\pi, 2^{-i-1}\pi]$, where $|\Theta_i(\omega)| = \sin(2^i\omega)$ and $|\Theta_i(\omega)| \geq |\Theta_i(2^{-5}\pi)|$. With these facts in mind and noting that $2^{i-4}|\Theta_4(\omega)| \leq 2^{i-4}$, we have

$$|\Theta_i(\omega)| \geq 2^{i-4}|\Theta_4(\omega)| \quad \forall \omega \in \left[2^{-5}\pi, 2^{-i-1}\pi\right]$$

which implies that

$$M_i(\omega) \geq 0, \quad \forall \omega \in \left[2^{-5}\pi, 2^{-i-1}\pi\right].$$

Thus, we arrive at $M_i(\omega) \geq 0$ for all $\omega \in [0, 2^{-i-1}\pi]$, which together with the fact $M_i(\omega) = M_i(-\omega)$ implies that $M_i(\omega) \geq 0$ for all $\omega \in [-2^{-i-1}\pi, 2^{-i-1}\pi]$. Furthermore, noting that $M_i(\omega)$ is a periodic function with a period $2^{-i}\pi$, we know $M_i(\omega) \geq 0$, that is, $|\Theta_i(\omega)| \geq 2^{i-4}|\Theta_4(\omega)|$ for all $\omega \in \mathbb{R}$ and $i = 1, \ldots, 4$. This completes the proof. ∎

Lemma 2: Let n_0 be an arbitrarily given positive integer. Consider $\Theta_i(\omega) = s_i \sin(2^i\omega)$ and define $\bar{\vartheta} = 2^{-5}\pi$ and $\vartheta_i = \sum_{i=1}^{4} 2^{-1-i}(s_i + 1)\pi$. Then, for all $k = 1, \ldots, 4$ and all $n = n_0, n_0 + 1, n_0 + 2, \ldots$

$$\Theta_i(\omega) \leq 0, \quad \forall \omega \in \left[n\pi + \vartheta_i, n\pi + \vartheta_i + 2\bar{\vartheta}\right],$$
$$\Theta_i\left(n\pi + \vartheta_i + \bar{\vartheta}\right) \leq -2^{-3}.$$

Proof: Define

$$n_i = \begin{cases} n, & \text{if } k = 1 \\ 2n_{i-1} + 0.5s_{i-1} + 0.5, & \text{if } k = 2, \ldots, 4 \end{cases}$$

where $n_1, \ldots, n_4$ are positive integers. If $s_i < 0$, then $\Theta_i(\omega) \leq 0$ when $\omega \in [2^{-i}(2n_i\pi), 2^{-i}(2n_i + 1)\pi]$. If $s_i \geq 0$, then $\Theta_i(\omega) \leq 0$ when $\omega \in [2^{-i}(2n_i + 1)\pi, 2^{-i}(2n_i + 2)\pi]$. Thus, we know $\Theta_i(\omega) \leq 0$ when $\omega \in \mathcal{I}_i$ with

$$\mathcal{I}_i = \left[2^{-i}(2n_i + 0.5s_i + 0.5)\pi, 2^{-i}(2n_i + 0.5s_i + 1.5)\pi\right].$$

It can be proved one by one that

$$\mathcal{I}_4 \subset \mathcal{I}_3 \subset \mathcal{I}_2 \subset \mathcal{I}_1$$

which implies that $\Theta_i(\omega) \leq 0$ when $\omega \in \mathcal{I}_4$ $\forall i = 1, \ldots, 4$. Moreover, n_4 can be calculated as

$$n_4 = 2^3 n + \sum_{i=1}^{3} 2^{3-i}(0.5s_i + 0.5).$$

Substituting n_4 into $\mathcal{I}_4$ gives

$$\mathcal{I}_4 = \left[n\pi + \vartheta_i, n\pi + \vartheta_i + 2\bar{\vartheta}\right].$$

Thus, $\Theta_i(\omega) \leq 0$ holds for $\forall \omega \in [n\pi + \vartheta_i, n\pi + \vartheta_i + 2\bar{\vartheta}]$. On the other hand, it can be readily checked that $\Theta_4(\omega) = -1$ when $\omega = 2^{-4}(2n_4 + 0.5s_4 + 1)\pi = n\pi + \vartheta_i + \bar{\vartheta}$, which, together with the last property in Lemma 1, implies that $|\Theta_i(n\pi + \vartheta_i + \bar{\vartheta})| \geq 2^{i-4}|\Theta_4(n\pi + \vartheta_i + \bar{\vartheta})| = 2^{i-4} \geq 2^{-3}$ for $i = 1, \ldots, 4$. Then, noting that $\Theta_i(n\pi + \vartheta_i + \bar{\vartheta}) \leq 0$, we can obtain that $\Theta_i(n\pi + \vartheta_i + \bar{\vartheta}) \leq -2^{-3}$. ∎

Lemma 3 [44]–[50]: Let $F(\boldsymbol{x})$ be a continuous function defined on a compact set $\Omega_{\boldsymbol{x}}$. Then, for a given desired level of accuracy $\varepsilon > 0$, there exists a fuzzy-logic system $\boldsymbol{W}^T \boldsymbol{\varphi}(\boldsymbol{x})$ such that

$$\sup_{\boldsymbol{x} \in \Omega_{\boldsymbol{x}}} \left|F(\boldsymbol{x}) - \boldsymbol{W}^T \boldsymbol{\varphi}(\boldsymbol{x})\right| \leq \varepsilon \tag{17}$$

where $\boldsymbol{\varphi}(\boldsymbol{x}) = [\phi_1(\boldsymbol{x}), \ldots, \phi_p(\boldsymbol{x})]^T$ is the fuzzy basis function vector, and

$$\phi_l(\boldsymbol{x}) = \frac{\prod_{j=1}^{m} \mu_{F_j^l}(x_j)}{\sum_{l=1}^{p}\left(\prod_{j=1}^{m} \mu_{F_j^l}(x_j)\right)} \tag{18}$$

with $\mu_{F_j^l}(x_j)$ being a fuzzy membership function of the variable x_j in If-Then rule. $\boldsymbol{W} = [w_1, \ldots, w_p]^T$ is the adaptive fuzzy parameter vector, and w_l is the inference variable corresponding to the lth If-Then rule. The optimal parameter vector $\boldsymbol{W}^*$ is defined as

$$\boldsymbol{W}^* = \arg \min_{\boldsymbol{W} \in \Omega_{\boldsymbol{W}}} \left\{ \sup_{\boldsymbol{x} \in \Omega_{\boldsymbol{x}}} \left|F(\boldsymbol{x}) - \boldsymbol{W}^T \boldsymbol{\varphi}(\boldsymbol{x})\right| \right\} \tag{19}$$

where $\Omega_{\boldsymbol{W}}$ is a compact set for $\boldsymbol{W}$.

Lemma 4 [30]: For any $q \in \mathbb{R}$ and $\forall \upsilon > 0$, the inequality $0 \leq |q| - (q^2/[\sqrt{q^2 + \upsilon^2}]) \leq \upsilon$ holds true.

III. FLIGHT CONTROLLER DESIGN

A. Velocity Control Design

In view of the decomposition of Section II-B, the control design is also decomposed in a velocity control design and an altitude control design (also refer to Fig. 3). Applying the error coordinate $\widetilde{V} = V - V_r$, an asymmetric IBLF is constructed as

$$\mathcal{L}_{\widetilde{V}} = \int_0^{\widetilde{V}} \frac{(k_{V,1} - k_{V,2})^2 \tau}{(k_{V,1} - \tau - V_r)(\tau + V_r - k_{V,2})} d\tau \tag{20}$$

where $k_{V,1}$ and $k_{V,2}$ are positive constants representing the upper and lower bounds of V, n., $k_{V,2} < V < k_{V,1}$. In view of (20), it can be immediately obtained that $\lim_{V \to k_{V,1}} \mathcal{L}_{\widetilde{V}} = +\infty$, $\lim_{V \to k_{V,2}} \mathcal{L}_{\widetilde{V}} = +\infty$, $\mathcal{L}_{\widetilde{V}} \geq (1/2)\widetilde{V}^2$, and $\mathcal{L}_{\widetilde{V}}$ is continuously differentiable and directly related to flight state V rather than its error $\widetilde{V}$.

Remark 2: The crucial discrepancy between IBLF (20) and other commonly seen BLFs as in [36] and [37] lies in that conventional BLFs are typically composed by error term $\widetilde{V}$ and transformed error constraints that still need to be calculated *a priori*, whereas IBLF (20) directly imposes constraint on original state V, which simplifies the control design in the sense of reducing extra calculations according to [39] and [40].

The following lemma is first formulated and is substantial in establishing constraint satisfaction.

Lemma 5: The asymmetric IBLF $\mathcal{L}_{\widetilde{V}}$ in (20) satisfies

$$\mathcal{L}_{\widetilde{V}} \leq \frac{(k_{V,1} - k_{V,2})^2 \widetilde{V}^2}{(k_{V,1} - V)(V - k_{V,2})} \tag{21}$$

for $V \in \Omega_0$.

Proof: Initially, define a function $\varsigma(\tau, V_r)$ as follows:

$$1_\varsigma(\tau, V_r) = \frac{(k_{V,1} - k_{V,2})^2 \tau}{(k_{V,1} - \tau - V_r)(\tau + V_r - k_{V,2})}.$$
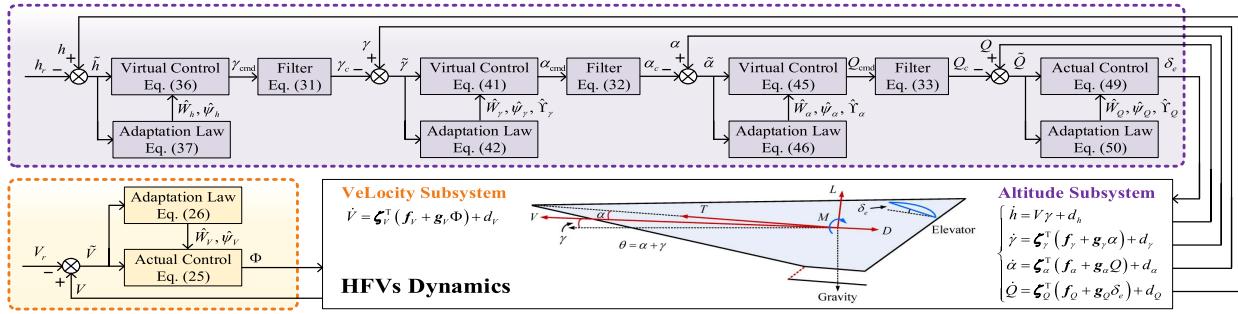
Fig. 3. Framework of the proposed control structure.

Differentiating $\varsigma(\tau, V_r)$ with respect to τ, we arrive at

$$\frac{\partial \varsigma(\tau, V_r)}{\partial \tau} = \frac{(k_{V,1} - k_{V,2})^2 \left[(k_{V,1} - V_r)(V_r - k_{V,2}) + \tau^2 \right]}{(k_{V,1} - \tau - V_r)^2 (\tau + V_r - k_{V,2})^2}$$

which is positive definite for $\tau + V_r \in \Omega_0$. Since $\varsigma(0, V_r) = 0$ for $V_r \in \Omega_0$, and $\varsigma(\tau, V_r)$ is monotonically increasing with respect to τ, the following inequality holds for $V \in \Omega_0$:

$$\int_0^{\widetilde{V}} \varsigma(\tau, V_r) \mathrm{d}\tau \leq \varsigma(\widetilde{V}, V_r) \widetilde{V}$$

which leads to (21) after substituting for $\varsigma(\tau, V_r)$. ∎

Differentiating $\mathcal{L}_{\widetilde{V}}$ with respect to time yields

$$\dot{\mathcal{L}}_{\widetilde{V}} = \frac{\partial \mathcal{L}_{\widetilde{V}}}{\partial \widetilde{V}} \dot{\widetilde{V}} + \frac{\partial \mathcal{L}_{\widetilde{V}}}{\partial V_r} \dot{V}_r \tag{22}$$

where $(\partial \mathcal{L}_{\widetilde{V}} / \partial \widetilde{V}) = \beta_V(V) \widetilde{V}$, $(\partial \mathcal{L}_{\widetilde{V}} / \partial V_r) = \beta_V(V) \widetilde{V} - \widetilde{V} \xi_V(\widetilde{V}, V_r)$ with $\xi_V(\widetilde{V}, V_r) = \int_0^1 ([(k_{V,1} - k_{V,2})^2] / [(k_{V,1} - \sigma \widetilde{V} - V_r)(\sigma \widetilde{V} + V_r - k_{V,2})]) \mathrm{d}\sigma$ and $\beta_V(V) = ([(k_{V,1} - k_{V,2})^2] / [(k_{V,1} - V)(V - k_{V,2})])$. By combining (13) and (22), one has

$$\dot{\mathcal{L}}_{\widetilde{V}} = s_1 g_1 \beta_V \widetilde{V} \Phi + \beta_V \widetilde{V} S_V(\boldsymbol{x}_V) + \beta_V \widetilde{V} d_V \tag{23}$$

where $S_V(\boldsymbol{x}_V) = \boldsymbol{\zeta}_V^T \boldsymbol{f}_V - \xi_V(\widetilde{V}, V_r) \dot{V}_r / \beta_V$ with $\boldsymbol{x}_V = [V, V_r, \dot{V}_r]^T$. According to Lemma 3, $S_V(\boldsymbol{x}_V)$ can be approximated by an FLS as $S_V(\boldsymbol{x}_V) = \boldsymbol{W}_V^{*T} \boldsymbol{\varphi}_V(\boldsymbol{x}_V) + \varepsilon_V$, where ε_V is the minimum fuzzy approximation error and there exists $\overline{\varepsilon}_V \in \mathbb{R}^+$ such that $|\varepsilon_V| \leq \overline{\varepsilon}_V$. Hence, we can obtain

$$\dot{\mathcal{L}}_{\widetilde{V}} \leq s_1 g_1 \beta_V \widetilde{V} \Phi + \beta_V \widetilde{V} \boldsymbol{W}_V^{*T} \boldsymbol{\varphi}_V(\boldsymbol{x}_V) + |\beta_V \widetilde{V}| \Psi_V \tag{24}$$

with $\Psi_V = \overline{d}_V + \overline{\varepsilon}_V$ being an unknown positive constant.

The actual controller for velocity channel is devised as

$$\Phi = \mathcal{N}_1(\omega_1) \phi_d, \quad \dot{\omega}_1 = \beta_V \widetilde{V} \phi_d$$

$$\phi_d = -\kappa_V \widetilde{V} - l_V \int_0^t \widetilde{V}(\tau) \mathrm{d}\tau$$

$$- \widehat{\boldsymbol{W}}_V^T \boldsymbol{\varphi}_V(\boldsymbol{x}_V) - \frac{\beta_V \widetilde{V} \widehat{\Psi}_V^2}{\sqrt{\beta_V^2 \widetilde{V}^2 \widehat{\Psi}_V^2 + \sigma^2}} \tag{25}$$

where $\mathcal{N}_1(\cdot)$ is given in (15), κ_V and l_V are positive design parameters, σ is a function satisfying $\int_0^t \sigma(\tau) \mathrm{d}\tau \leq \sigma_1 < \infty$ and $\sigma_1 > 0$ $\forall t \in (0, +\infty)$, $\widehat{\boldsymbol{W}}_V$ is the estimate of $\boldsymbol{W}_V^*$ with estimation error $\widetilde{\boldsymbol{W}}_V = \boldsymbol{W}_V^* - \widehat{\boldsymbol{W}}_V$.

The adaptation laws are given by

$$\dot{\widehat{\boldsymbol{W}}}_V = \Gamma_V \beta_V \widetilde{V} \boldsymbol{\varphi}_V(\boldsymbol{x}_V) - \sigma \Gamma_V \widehat{\boldsymbol{W}}_V$$

$$\dot{\widehat{\Psi}}_V = \rho_V |\beta_V \widetilde{V}| - \sigma \rho_V \widehat{\Psi}_V \tag{26}$$

where $\Gamma_V = \Gamma_V^T > 0$ is an adaption gain matrix, and ρ_V is a positive design parameter.

Substituting (25) into (24), we arrive at

$$\dot{\mathcal{L}}_{\widetilde{V}} \leq -\kappa_V \beta_V \widetilde{V}^2 - l_V \beta_V \widetilde{V} \int_0^t \widetilde{V}(\tau) \mathrm{d}\tau + s_1 g_1 \mathcal{N}_1(\omega_1) \dot{\omega}_1$$

$$- \dot{\omega}_1 + |\beta_V \widetilde{V}| \Psi_V - \frac{\beta_V^2 \widetilde{V}^2 \widehat{\Psi}_V^2}{\sqrt{\beta_V^2 \widetilde{V}^2 \widehat{\Psi}_V^2 + \sigma^2}}$$

$$+ \beta_V \widetilde{V} \widetilde{\boldsymbol{W}}_V^T \boldsymbol{\varphi}_V(\boldsymbol{x}_V). \tag{27}$$

B. Altitude Control Design

Step 1: Using the error coordinate $\widetilde{h} = h - h_r$, the asymmetric IBLF is constructed as

$$\mathcal{L}_{\widetilde{h}} = \int_0^{\widetilde{h}} \frac{(k_{h,1} - k_{h,2})^2 \tau}{(k_{h,1} - \tau - h_r)(\tau + h_r - k_{h,2})} \mathrm{d}\tau \tag{28}$$

where $k_{h,1}$ and $k_{h,2}$ are positive constants representing the upper and lower bounds of h, that is, $k_{h,2} < h < k_{h,1}$. It is straightforward to obtain that (28) satisfies $\lim_{h \to k_{h,1}} \mathcal{L}_{\widetilde{h}} = +\infty$, $\lim_{h \to k_{h,2}} \mathcal{L}_{\widetilde{h}} = +\infty$, and $\mathcal{L}_{\widetilde{h}} \geq (1/2) \widetilde{h}^2$. Similar to Lemma 5, one has $\mathcal{L}_{\widetilde{h}} \leq ([(k_{h,1} - k_{h,2})^2 \widetilde{h}^2] / [(k_{h,1} - h)(h - k_{h,2})])$.

Then, the time derivative of $\mathcal{L}_{\widetilde{h}}$ is

$$\dot{\mathcal{L}}_{\widetilde{h}} = \frac{\partial \mathcal{L}_{\widetilde{h}}}{\partial \widetilde{h}} \dot{\widetilde{h}} + \frac{\partial \mathcal{L}_{\widetilde{h}}}{\partial h_r} \dot{h}_r \tag{29}$$

where $(\partial \mathcal{L}_{\widetilde{h}} / \partial \widetilde{h}) = \beta_h(h) \widetilde{h}$, $(\partial \mathcal{L}_{\widetilde{h}} / \partial h_r) = \beta_h(h) \widetilde{h} - \widetilde{h} \xi_h(\widetilde{h}, h_r)$, with $\xi_h(\widetilde{h}, h_r) = \int_0^1 ([(k_{h,1} - k_{h,2})^2] / [(k_{h,1} - \sigma \widetilde{h} - h_r)(\sigma \widetilde{h} + h_r - k_{h,2})]) \mathrm{d}\sigma$ and $\beta_h(h) = ([(k_{h,1} - k_{h,2})^2] / [(k_{h,1} - h)(h - k_{h,2})])$.

To avoid the "explosion of complexity" problem, we follow a standard dynamic surface control method appropriately modified to the purpose of differentiability [51]. Let us consider the coordinate transformation

$$\begin{cases} \widetilde{\gamma} = \gamma - \gamma_c, & y_\gamma = \gamma_c - \gamma_{\mathrm{cmd}} \\ \widetilde{\alpha} = \alpha - \alpha_c, & y_\alpha = \alpha_c - \alpha_{\mathrm{cmd}} \\ \widetilde{Q} = Q - Q_c, & y_Q = Q_c - Q_{\mathrm{cmd}} \end{cases} \tag{30}$$

where $\widetilde{\gamma}$, $\widetilde{\alpha}$, and $\widetilde{Q}$ are the tracking errors, γ_{cmd}, α_{cmd}, and Q_{cmd} are the virtual control laws, y_γ, y_α, and y_Q are the boundary layer errors, and γ_c, α_c, and Q_c are the outputs of the following first-order filters:

$$\tau_\gamma \dot{\gamma}_c = -y_\gamma - \frac{\tau_\gamma y_\gamma \widehat{\Upsilon}_\gamma^2}{\sqrt{y_\gamma^2 \widehat{\Upsilon}_\gamma^2 + \sigma^2}} \tag{31}$$

$$\tau_\alpha \dot{\alpha}_c = -y_\alpha - \frac{\tau_\alpha y_\alpha \widehat{\Upsilon}_\alpha^2}{\sqrt{y_\alpha^2 \widehat{\Upsilon}_\alpha^2 + \sigma^2}} \tag{32}$$

$$\tau_Q \dot{Q}_c = -y_Q - \frac{\tau_Q y_Q \widehat{\Upsilon}_Q^2}{\sqrt{y_Q^2 \widehat{\Upsilon}_Q^2 + \sigma^2}} \tag{33}$$

where τ_γ, τ_α, and τ_Q are positive constants, $\widehat{\Upsilon}_z$ is estimate of Υ_z, $z \in \Omega_z \triangleq \{\gamma, \alpha, Q\}$, which will be specified later.

From Young's inequality [52], it follows that $s_2 \beta_h \widetilde{h} V y_\gamma \leq ([\beta_h^2 \widetilde{h}^2 V^2]/[2l_h^2]) + ([y_\gamma^2 l_h^2]/2)$. Then, by combining (14) and (29), it yields

$$\dot{\mathcal{L}}_{\widetilde{h}} \leq \beta_h \widetilde{h} V(\widetilde{\gamma} + \gamma_{\text{cmd}}) + \beta_h \widetilde{h} S_h(\boldsymbol{x}_h) + \beta_h \widetilde{h} d_h + \frac{y_\gamma^2 l_h^2}{2} \tag{34}$$

where $S_h(\boldsymbol{x}_h) = ([\beta_h \widetilde{h} V^2]/[2l_h^2]) - ([\xi_h \dot{h}_r]/[\beta_h])$ with $\boldsymbol{x}_h = [h, h_r, \dot{h}_r]^T$. According to Lemma 3, $S_h(\boldsymbol{x}_h)$ can be approximated by an FLS as $S_h(\boldsymbol{x}_h) = \boldsymbol{W}_h^{*T} \boldsymbol{\varphi}_h(\boldsymbol{x}_h) + \varepsilon_h$, where ε_h is the minimum fuzzy approximation error and there exists $\overline{\varepsilon}_h \in \mathbb{R}^+$ such that $|\varepsilon_h| \leq \overline{\varepsilon}_h$. Thus, it holds that

$$\dot{\mathcal{L}}_{\widetilde{h}} \leq \beta_h \widetilde{h} V(\widetilde{\gamma} + \gamma_{\text{cmd}}) + \beta_h \widetilde{h} \boldsymbol{W}_h^{*T} \boldsymbol{\varphi}_h(\boldsymbol{x}_h) + |\beta_h \widetilde{h}| \Psi_h + \frac{y_\gamma^2 l_h^2}{2} \tag{35}$$

with $\Psi_h = \overline{d}_h + \overline{\varepsilon}_h$ being an unknown positive constant.

The virtual controller γ_{cmd} is devised as

$$\gamma_{\text{cmd}} = \frac{1}{V} \left\{ -\kappa_h \widetilde{h} - l_h \int_0^t \widetilde{h}(\tau) \mathrm{d}\tau \right.$$
$$\left. - \widehat{\boldsymbol{W}}_h^T \boldsymbol{\varphi}_h(\boldsymbol{x}_h) - \frac{\beta_h \widetilde{h} \widehat{\Psi}_h^2}{\sqrt{\beta_h^2 \widetilde{h}^2 \widehat{\Psi}_h^2 + \sigma^2}} \right\} \tag{36}$$

where κ_h and l_h are positive design parameters, and $\widehat{\boldsymbol{W}}_h$ is the estimate of $\boldsymbol{W}_h^*$ with estimation error $\widetilde{\boldsymbol{W}}_h = \boldsymbol{W}_h^* - \widehat{\boldsymbol{W}}_h$.

The adaptation laws are given by

$$\dot{\widehat{\boldsymbol{W}}}_h = \Gamma_h \beta_h \widetilde{h} \boldsymbol{\varphi}_h(\boldsymbol{x}_h) - \sigma \Gamma_h \widehat{\boldsymbol{W}}_h$$
$$\dot{\widehat{\Psi}}_h = \rho_h |\beta_h \widetilde{h}| - \sigma \rho_h \widehat{\Psi}_h \tag{37}$$

where $\Gamma_h = \Gamma_h^T > 0$ is an adaption gain matrix, and ρ_h is a positive design parameter.

Substituting (36) into (35) yields

$$\dot{\mathcal{L}}_{\widetilde{h}} \leq -\kappa_h \beta_h \widetilde{h}^2 - l_h \beta_h \widetilde{h} \int_0^t \widetilde{h}(\tau) \mathrm{d}\tau + \beta_h \widetilde{h} \widetilde{\boldsymbol{W}}_h^T \boldsymbol{\varphi}_h(\boldsymbol{x}_h)$$
$$+ |\beta_h \widetilde{h}| \Psi_h - \frac{\beta_h^2 \widetilde{h}^2 \widehat{\Psi}_h^2}{\sqrt{\beta_h^2 \widetilde{h}^2 \widehat{\Psi}_h^2 + \sigma^2}} + \frac{y_\gamma^2 l_h^2}{2} + \beta_h \widetilde{h} V \widetilde{\gamma}. \tag{38}$$

Step 2: Using the error coordinate (30), the asymmetric IBLF is constructed as

$$\mathcal{L}_{\widetilde{\gamma}} = \int_0^{\widetilde{\gamma}} \frac{(k_{\gamma,1} + k_{\gamma,2})^2 \tau}{(k_{\gamma,1} - \tau - \gamma_c)(\tau + \gamma_c + k_{\gamma,2})} \mathrm{d}\tau \tag{39}$$

where $k_{\gamma,1}$ and $k_{\gamma,2}$ are positive constants denoting the upper and lower bounds of γ, that is, $-k_{\gamma,2} < \gamma < k_{\gamma,1}$. Similarly, the IBLF defined in (39) satisfies $\lim_{\gamma \to -k_{\gamma,2}} \mathcal{L}_{\widetilde{\gamma}} =$

$+\infty$, $\lim_{\gamma \to k_{\gamma,1}} \mathcal{L}_{\widetilde{\gamma}} = +\infty$, $\mathcal{L}_{\widetilde{\gamma}} \geq (1/2)\widetilde{\gamma}^2$, and $\mathcal{L}_{\widetilde{\gamma}} \leq ([(k_{\gamma,1} + k_{\gamma,2})^2 \widetilde{\gamma}^2]/[(k_{\gamma,1} - \gamma)(\gamma + k_{\gamma,2})])$.

Taking the time derivative of $\mathcal{L}_{\widetilde{\gamma}}$ gives

$$\dot{\mathcal{L}}_{\widetilde{\gamma}} = \frac{\partial \mathcal{L}_{\widetilde{\gamma}}}{\partial \widetilde{\gamma}} \dot{\widetilde{\gamma}} + \frac{\partial \mathcal{L}_{\widetilde{\gamma}}}{\partial \gamma_c} \dot{\gamma}_c \tag{40}$$

where $(\partial \mathcal{L}_{\widetilde{\gamma}}/\partial \widetilde{\gamma}) = \beta_\gamma(\gamma)\widetilde{\gamma}$, $(\partial \mathcal{L}_{\widetilde{\gamma}}/\partial \gamma_c) = \beta_\gamma(\gamma)\widetilde{\gamma} - \widetilde{\gamma}\xi_\gamma(\widetilde{\gamma}, \gamma_c)$ with $\xi_\gamma(\widetilde{\gamma}, \gamma_c) = \int_0^1 ([(k_{\gamma,1} + k_{\gamma,2})^2]/[(k_{\gamma,1} - \sigma\widetilde{\gamma} - \gamma_c)(\sigma\widetilde{\gamma} + \gamma_c + k_{\gamma,2})])\mathrm{d}\sigma$ and $\beta_\gamma(\gamma) = ([(k_{\gamma,1} + k_{\gamma,2})^2]/[(k_{\gamma,1} - \gamma)(\gamma + k_{\gamma,2})])$.

The virtual controller α_{cmd} is devised as

$$\alpha_{\text{cmd}} = \mathcal{N}_2(\omega_2)\alpha_d, \quad \dot{\omega}_2 = \beta_\gamma \widetilde{\gamma} \alpha_d$$
$$\alpha_d = -\kappa_\gamma \widetilde{\gamma} - l_\gamma \int_0^t \widetilde{\gamma}(\tau) \mathrm{d}\tau$$
$$- \widehat{\boldsymbol{W}}_\gamma^T \boldsymbol{\varphi}_\gamma(\boldsymbol{x}_\gamma) - \frac{\beta_\gamma \widetilde{\gamma} \widehat{\Psi}_\gamma^2}{\sqrt{\beta_\gamma^2 \widetilde{\gamma}^2 \widehat{\Psi}_\gamma^2 + \sigma^2}} \tag{41}$$

where $\boldsymbol{x}_\gamma = [h, \gamma, \gamma_c, \dot{\gamma}_c]^T$, $\mathcal{N}_2(\cdot)$ is given in (15), κ_γ and l_γ are positive design parameters.

The adaptation laws are given by

$$\dot{\widehat{\boldsymbol{W}}}_\gamma = \Gamma_\gamma \beta_\gamma \widetilde{\gamma} \boldsymbol{\varphi}_\gamma(\boldsymbol{x}_\gamma) - \sigma \Gamma_\gamma \widehat{\boldsymbol{W}}_\gamma$$
$$\dot{\widehat{\Psi}}_\gamma = \rho_\gamma |\beta_\gamma \widetilde{\gamma}| - \sigma \rho_\gamma \widehat{\Psi}_\gamma$$
$$\dot{\widehat{\Upsilon}}_\gamma = \upsilon_\gamma |y_\gamma| - \sigma \upsilon_\gamma \widehat{\Upsilon}_\gamma \tag{42}$$

where $\Gamma_\gamma = \Gamma_\gamma^T > 0$ is an adaption gain matrix, and ρ_γ and υ_γ are positive design parameters.

Substituting (41) into (40), we arrive at

$$\dot{\mathcal{L}}_{\widetilde{\gamma}} \leq -\kappa_\gamma \beta_\gamma \widetilde{\gamma}^2 - l_\gamma \beta_\gamma \widetilde{\gamma} \int_0^t \widetilde{\gamma}(\tau) \mathrm{d}\tau + s_2 g_2 \mathcal{N}_2(\omega_2)\dot{\omega}_2$$
$$+ |\beta_\gamma \widetilde{\gamma}| \Psi_\gamma - \frac{\beta_\gamma^2 \widetilde{\gamma}^2 \widehat{\Psi}_\gamma^2}{\sqrt{\beta_\gamma^2 \widetilde{\gamma}^2 \widehat{\Psi}_\gamma^2 + \sigma^2}} + \frac{y_\alpha^2 l_\gamma^2}{2} - \beta_h \widetilde{h} V \widetilde{\gamma}$$
$$+ \beta_\gamma \widetilde{\gamma} \widetilde{\boldsymbol{W}}_\gamma^T \boldsymbol{\varphi}_\gamma(\boldsymbol{x}_\gamma) + s_2 g_2 \beta_\gamma \widetilde{\gamma} \widetilde{\alpha} - \dot{\omega}_2. \tag{43}$$

Step 3: Recalling the error coordinate (30), the asymmetric IBLF is constructed as

$$\mathcal{L}_{\widetilde{\alpha}} = \int_0^{\widetilde{\alpha}} \frac{(k_{\alpha,1} + k_{\alpha,2})^2 \tau}{(k_{\alpha,1} - \tau - \alpha_c)(\tau + \alpha_c + k_{\alpha,2})} \mathrm{d}\tau \tag{44}$$

where $k_{\alpha,1}$ and $k_{\alpha,2}$ are positive constants representing the upper and lower bounds of α, that is, $-k_{\alpha,2} < \alpha < k_{\alpha,1}$.

The virtual controller Q_{cmd} is devised as

$$Q_{\text{cmd}} = \mathcal{N}_3(\omega_3)Q_d, \quad \dot{\omega}_3 = \beta_\alpha \widetilde{\alpha} Q_d$$
$$Q_d = -\kappa_\alpha \widetilde{\alpha} - l_\alpha \int_0^t \widetilde{\alpha}(\tau) \mathrm{d}\tau$$
$$- \widehat{\boldsymbol{W}}_\alpha^T \boldsymbol{\varphi}_\alpha(\boldsymbol{x}_\alpha) - \frac{\beta_\alpha \widetilde{\alpha} \widehat{\Psi}_\alpha^2}{\sqrt{\beta_\alpha^2 \widetilde{\alpha}^2 \widehat{\Psi}_\alpha^2 + \sigma^2}} \tag{45}$$

where $\boldsymbol{x}_\alpha = [h, \gamma, \alpha, \alpha_c, \dot{\alpha}_c]^T$, $\mathcal{N}_3(\cdot)$ is given in (15), and κ_α and l_α are positive design parameters.

The adaptation laws are given by

$$\dot{\widehat{\boldsymbol{W}}}_\alpha = \Gamma_\alpha \beta_\alpha \widetilde{\alpha} \boldsymbol{\varphi}_\alpha(\boldsymbol{x}_\alpha) - \sigma \Gamma_\alpha \widehat{\boldsymbol{W}}_\alpha$$

$$\dot{\widehat{\Psi}}_\alpha = \rho_\alpha |\beta_\alpha \widetilde{\alpha}| - \sigma \rho_\alpha \widehat{\Psi}_\alpha$$
$$\dot{\widehat{\Upsilon}}_\alpha = \upsilon_\alpha |y_\alpha| - \sigma \upsilon_\alpha \widehat{\Upsilon}_\alpha \qquad (46)$$

where $\Gamma_\alpha = \Gamma_\alpha^T > 0$ is an adaption gain matrix, and ρ_α and υ_α are positive design parameters.

Substituting (45) into (44) results in

$$\dot{\mathcal{L}}_{\widetilde{\alpha}} \leq -\kappa_\alpha \beta_\alpha \widetilde{\alpha}^2 - l_\alpha \beta_\alpha \widetilde{\alpha} \int_0^t \widetilde{\alpha}(\tau) d\tau + s_3 g_3 \mathcal{N}_3(\omega_3) \dot{\omega}_3$$
$$+ |\beta_\alpha \widetilde{\alpha}| \Psi_\alpha - \frac{\beta_\alpha^2 \widetilde{\alpha}^2 \widehat{\Psi}_\alpha^2}{\sqrt{\beta_\alpha^2 \widetilde{\alpha}^2 \widehat{\Psi}_\alpha^2 + \sigma^2}} + \frac{y_Q^2 l_\alpha^2}{2} - s_2 g_2 \beta_\gamma \widetilde{\gamma} \widetilde{\alpha}$$
$$+ \beta_\alpha \widetilde{\alpha} \widetilde{W}_\alpha^T \varphi_\alpha(x_\alpha) + s_3 g_3 \beta_\alpha \widetilde{\alpha} Q - \dot{\omega}_3. \qquad (47)$$

Step 4: Along similar lines as steps former steps, the asymmetric IBLF is constructed as

$$\mathcal{L}_{\widetilde{Q}} = \int_0^{\widetilde{Q}} \frac{(k_{Q,1} + k_{Q,2})^2 \tau}{(k_{Q,1} - \tau - Q_c)(\tau + Q_c + k_{Q,2})} d\tau \qquad (48)$$

where $k_{Q,1}$ and $k_{Q,2}$ are positive constants denoting the upper and lower bounds of Q, that is, $-k_{Q,2} < Q < k_{Q,1}$.

The actual controller δ_e is constructed as

$$\delta_e = \mathcal{N}_4(\omega_4) \delta_d, \quad \dot{\omega}_4 = \beta_Q \widetilde{Q} \delta_d$$
$$\delta_d = -\kappa_Q \widetilde{Q} - l_Q \int_0^t \widetilde{Q}(\tau) d\tau$$
$$- \widehat{W}_Q^T \varphi_Q(x_Q) - \frac{\beta_Q \widetilde{Q} \widehat{\Psi}_Q^2}{\sqrt{\beta_Q^2 \widetilde{Q}^2 \widehat{\Psi}_Q^2 + \sigma^2}} \qquad (49)$$

where $x_Q = [h, \gamma, \alpha, Q, Q_c, \dot{Q}_c]^T$, $\mathcal{N}_4(\cdot)$ is given in (15), and κ_Q and l_Q are positive design parameters.

The adaptation laws are given by

$$\dot{\widehat{W}}_Q = \Gamma_Q \beta_Q \widetilde{Q} \varphi_Q(x_Q) - \sigma \Gamma_Q \widehat{W}_Q$$
$$\dot{\widehat{\Psi}}_Q = \rho_Q |\beta_Q \widetilde{Q}| - \sigma \rho_Q \widehat{\Psi}_Q$$
$$\dot{\widehat{\Upsilon}}_Q = \upsilon_Q |y_Q| - \sigma \upsilon_Q \widehat{\Upsilon}_Q \qquad (50)$$

where $\Gamma_Q = \Gamma_Q^T > 0$ is an adaption gain matrix, and ρ_Q and υ_Q are positive design parameters.

It follows from (48) and (49) that:

$$\dot{\mathcal{L}}_{\widetilde{Q}} \leq -\kappa_Q \beta_Q \widetilde{Q}^2 - l_Q \beta_Q \widetilde{Q} \int_0^t \widetilde{Q}(\tau) d\tau + s_4 g_4 \mathcal{N}_4(\omega_4) \dot{\omega}_4$$
$$+ |\beta_Q \widetilde{Q}| \Psi_Q - \frac{\beta_Q^2 \widetilde{Q}^2 \widehat{\Psi}_Q^2}{\sqrt{\beta_Q^2 \widetilde{Q}^2 \widehat{\Psi}_Q^2 + \sigma^2}} - s_3 g_3 \beta_\alpha \widetilde{\alpha} \widetilde{Q}$$
$$+ \beta_Q \widetilde{Q} \widetilde{W}_Q^T \varphi_Q(x_Q) - \dot{\omega}_4. \qquad (51)$$

IV. STABILITY ANALYSIS

We are at the position to present the main results of this study in the following theorem.

Theorem 1: Consider the closed-loop systems consisting of velocity dynamics (13) and altitude dynamics (14) subject to multiple unknown control directions and asymmetric flight state constraints. Under the control laws (25), (36), (41), (45), and (49), as well as the adaptation laws (26), (37), (42), (46), and (50), for any initial condition

$x(0) \in \Omega_0$, $x \in \Omega_x \triangleq \{V, h, \gamma, \alpha, Q\}$ and let $A_\gamma = \max |\gamma_c(\widetilde{h}, y_\gamma, \widehat{W}_h, \widehat{\Psi}_h)|$, $A_\alpha = \max |\alpha_c(\widetilde{h}, \widetilde{\gamma}, y_\alpha, \widehat{W}_\gamma, \widehat{\Psi}_\gamma)|$, $A_Q = \max |Q_c(\widetilde{h}, \widetilde{\gamma}, \widetilde{\alpha}, y_Q, \widehat{W}_\alpha, \widehat{\Psi}_\alpha)|$, if there are the positive parameters $\kappa_h, l_h, \kappa_\gamma, l_\gamma, \kappa_\alpha$, and l_α that satisfy the feasibility condition: $-k_{\gamma,2} < A_\gamma(\kappa_h, l_h) < k_{\gamma,1}$, $-k_{\alpha,2} < A_\alpha(\kappa_\gamma, l_\gamma) < k_{\alpha,1}$, and $-k_{Q,2} < A_Q(\kappa_\alpha, l_\alpha) < k_{Q,1}$, then the following properties hold.

1) Flight states V and h eventually track the reference trajectories V_r and h_r asymptotically, that is, $\widetilde{V} \to 0$ and $\widetilde{h} \to 0$ as $t \to \infty$.
2) All closed-loop signals remain bounded.
3) The full-state constraints are never violated.

Proof: We begin the proof with the introduction of the following total Lyapunov function:

$$\mathcal{L} = \mathcal{L}_s + \mathcal{L}_W + \mathcal{L}_y + \mathcal{L}_\Psi + \mathcal{L}_\Upsilon + \mathcal{L}_l \qquad (52)$$

where $\mathcal{L}_s = \sum_{x \in \Omega_x} \mathcal{L}_{\widetilde{x}}$, $\mathcal{L}_W = \sum_{x \in \Omega_x} (1/2) \widetilde{W}_x^T \Gamma_x^{-1} \widetilde{W}_x$, $\mathcal{L}_y = \sum_{z \in \Omega_z} (1/2) y_z^2$, $\mathcal{L}_\Psi = \sum_{x \in \Omega_x} (1/2\rho_x) \widetilde{\Psi}_x^2$, $\mathcal{L}_\Upsilon = \sum_{z \in \Omega_z} (1/2\upsilon_z) \widetilde{\Upsilon}_z^2$, and $\mathcal{L}_l = \sum_{x \in \Omega_x} (1/2) l_x \beta_x (\int_0^t \widetilde{x}(\tau) d\tau)^2$.

It follows from (27), (38), (43), (47), and (51) that the derivative of $\mathcal{L}$ is:

$$\dot{\mathcal{L}} \leq - \sum_{x \in \Omega_x} \kappa_x \beta_x \widetilde{x}^2 + \sum_{i=1}^4 s_i g_i \mathcal{N}_i(\omega_i) \dot{\omega}_i + \sum_{x \in \Omega_x} |\beta_x \widetilde{x}| \widehat{\Psi}_x$$
$$+ \sum_{x \in \Omega_x} \sigma \widetilde{W}_x \widehat{W}_x + \sum_{x \in \Omega_x} \sigma \widetilde{\Psi}_x \widehat{\Psi}_x + \sum_{z \in \Omega_z} \sigma \widetilde{\Upsilon}_z \widehat{\Upsilon}_z$$
$$- \sum_{x \in \Omega_x} \frac{\beta_x^2 \widetilde{x}^2 \widehat{\Psi}_x^2}{\sqrt{\beta_x^2 \widetilde{x}^2 \widehat{\Psi}_x^2 + \sigma^2}} - \sum_{i=1}^4 \dot{\omega}_i - \sum_{z \in \Omega_z} |y_z| \widetilde{\Upsilon}_z$$
$$+ \sum_{z \in \Omega_z} y_z \dot{y}_z + \frac{y_\gamma^2 l_h^2}{2} + \frac{y_\alpha^2 l_\gamma^2}{2} + \frac{y_Q^2 l_\alpha^2}{2}. \qquad (53)$$

In light of (36), (41), and (45), the time derivatives of the boundary layer errors are

$$\dot{y}_\gamma = B_\gamma \left(\widetilde{h}, \widetilde{\gamma}, y_\gamma, \widehat{W}_h, \widehat{\Psi}_h, h_r, \dot{h}_r, \ddot{h}_r, \sigma, \dot{\sigma} \right)$$
$$- \frac{y_\gamma}{\tau_\gamma} - \frac{y_\gamma \widehat{\Upsilon}_h^2}{\sqrt{y_\gamma^2 \widehat{\Upsilon}_h^2 + \sigma^2}} \qquad (54)$$

$$\dot{y}_\alpha = B_\alpha \left(\widetilde{h}, \widetilde{\gamma}, \widetilde{\alpha}, y_\gamma, y_\alpha, \widehat{W}_h, \widehat{W}_\gamma, \widehat{\Psi}_h, \widehat{\Psi}_\gamma, h_r, \dot{h}_r, \ddot{h}_r, \sigma, \dot{\sigma} \right)$$
$$- \frac{y_\alpha}{\tau_\alpha} - \frac{y_\alpha \widehat{\Upsilon}_\gamma^2}{\sqrt{y_\alpha^2 \widehat{\Upsilon}_\gamma^2 + \sigma^2}} \qquad (55)$$

$$\dot{y}_Q = B_Q \left(\widetilde{h}, \widetilde{\gamma}, \widetilde{\alpha}, \widetilde{Q}, y_\gamma, y_\alpha, y_Q, \widehat{W}_h, \widehat{W}_\gamma, \widehat{W}_\alpha, \widehat{\Psi}_h, \widehat{\Psi}_\gamma, \widehat{\Psi}_\alpha \right.$$
$$\left. h_r, \dot{h}_r, \ddot{h}_r, \sigma, \dot{\sigma} \right) - \frac{y_Q}{\tau_Q} - \frac{y_Q \widehat{\Upsilon}_\alpha^2}{\sqrt{y_Q^2 \widehat{\Upsilon}_\alpha^2 + \sigma^2}}. \qquad (56)$$

Define the compact sets $\Omega_r' = \{h_r^{(n)}, V_r^{(n)} | |h_r^{(n)}| \leq \Delta_1, |V_r^{(n)}| \leq \Delta_1, n \in \mathbb{N}\}$ and $\Omega_{\mathcal{L}} = \{\widetilde{x}, \widetilde{W}_x, y_z, \Psi_x, \widetilde{\Upsilon}_z | \mathcal{L}(t) \leq \Delta_0, x \in \Omega_x, z \in \Omega_z\}$, with Δ_1 and Δ_0 being positive constants. Following the standard design in [51], it can be derived that there exist positive constants Υ_γ, Υ_α, and Υ_Q such that $B_\gamma(\cdot) \leq \Upsilon_\gamma$, $B_\alpha(\cdot) \leq \Upsilon_\alpha$, and $B_Q(\cdot) \leq \Upsilon_Q$ on the compact set

$\Omega'_r \times \Omega_{\mathcal{L}}$. Then, (53) can be further rewritten as

$$
\begin{aligned}
\dot{\mathcal{L}} \leq & -\sum_{x \in \Omega_x} \kappa_x \beta_x \widetilde{x}^2 + \sum_{i=1}^{4} s_i g_i \mathcal{N}_i(\omega_i) \dot{\omega}_i + \sum_{z \in \Omega_z} |y_z| \widehat{\Upsilon}_z \\
& - \sum_{x \in \Omega_x} \frac{\beta_x^2 \widetilde{x}^2 \widehat{\Psi}_x^2}{\sqrt{\beta_x^2 \widetilde{x}^2 \widehat{\Psi}_x^2 + \sigma^2}} + \sum_{x \in \Omega_x} |\beta_x \widetilde{x}| \widehat{\Psi}_x - \sum_{i=1}^{4} \dot{\omega}_i \\
& - \frac{y_\gamma^2 \widehat{\Upsilon}_h^2}{\sqrt{y_\gamma^2 \widehat{\Upsilon}_h^2 + \sigma^2}} - \frac{y_\alpha^2 \widehat{\Upsilon}_\gamma^2}{\sqrt{y_\alpha^2 \widehat{\Upsilon}_\gamma^2 + \sigma^2}} - \frac{y_Q^2 \widehat{\Upsilon}_\alpha^2}{\sqrt{y_Q^2 \widehat{\Upsilon}_\alpha^2 + \sigma^2}} \\
& - \left(\frac{1}{\tau_\gamma} - \frac{l_h^2}{2}\right) y_\gamma^2 - \left(\frac{1}{\tau_\alpha} - \frac{l_\gamma^2}{2}\right) y_\alpha^2 - \left(\frac{1}{\tau_Q} - \frac{l_\alpha^2}{2}\right) y_Q^2 \\
& + \sum_{x \in \Omega_x} \sigma \widetilde{W}_x \widehat{W}_x + \sum_{x \in \Omega_x} \sigma \widetilde{\Psi}_x \widehat{\Psi}_x + \sum_{z \in \Omega_z} \sigma \widetilde{\Upsilon}_z \widehat{\Upsilon}_z. \quad (57)
\end{aligned}
$$

Using the complete square formula, we have $\widetilde{x} \widehat{x} = \widetilde{x}(x^* - \widetilde{x}) = -\widetilde{x}^2 + \widetilde{x} x^* \leq (1/4)x^*$. Thus, invoking Lemma 4 and choosing $\tau_\gamma < (2/l_h^2)$, $\tau_\alpha < (2/l_\gamma^2)$, and $\tau_Q < (2/l_\alpha^2)$ gives rise to

$$
\begin{aligned}
\mathcal{L}(t) \leq & -F(t) + \sum_{i=1}^{4} \int_0^{\omega_i(t)} s_i g_i \mathcal{N}_i(\tau) d\tau - \sum_{i=1}^{4} \omega_i(t) \\
& + \mathcal{L}(0) + M \quad (58)
\end{aligned}
$$

where $F(t) = \int_0^t (1/2)(\kappa_V \widetilde{V}^2(\tau) + \kappa_h \widetilde{h}^2(\tau) + \kappa_\gamma \widetilde{\gamma}^2(\tau) + \kappa_\alpha \widetilde{\alpha}^2(\tau) + \kappa_Q \widetilde{Q}^2(\tau)) d\tau$ and $M = \sum_{x \in \Omega_x} (1/4)\sigma_1 W_x^* + \sum_{x \in \Omega_x}(1/4)\sigma_1 \Psi_x + \sum_{z \in \Omega_z}(1/4)\sigma_1 \Upsilon_z - \sum_{i=1}^{4} \int_0^{\omega_i(0)} s_i g_i \mathcal{N}_i(\tau) d\tau + \sum_{i=1}^{4} \omega_i(0) + 8\sigma_1$. It can be seen from (16) that $\int_0^{\omega_i} \mathcal{N}_i(\tau) d\tau = \int_0^{|\omega_i|} \mathcal{N}_i(\tau) d\tau = s_i \Theta_i(|\omega_i|) |\omega_i| \exp(\omega_i^2)$. As a result, (58) can be represented by

$$
0 \leq \mathcal{L}(t) + F(t) \leq \mathcal{L}(0) + M + \sum_{i=1}^{4} \Xi_i(t) + \sum_{i=1}^{4} |\omega_i(t)| \quad (59)
$$

with $\Xi_i(t) = g_i \Theta_i(|\omega_i(t)|) |\omega_i(t)| \exp(\omega_i^2(t))$.

Let us now define

$$
\overline{\omega}(t) = \max\{|\omega_1(t)|, |\omega_2(t)|, |\omega_3(t)|, |\omega_4(t)|\}. \quad (60)
$$

In what follows, with the aid of Lemma 1 and (59), we shall prove the boundedness of $\overline{\omega}(t)$ via a contradiction argument. Choose n_0 in Lemma 2 as the smallest positive integer satisfying $n_0 \pi + \vartheta_i + \bar{\vartheta} \geq \overline{\omega}(0)$ for all $i = 1, \ldots, 4$, where ϑ_i and $\bar{\vartheta}$ are given in Lemma 2. Suppose that $\overline{\omega}(t)$ is unbounded, which is equivalent to that there exists a monotonously increasing sequence $\{t_n\}$, $n = n_0, n_0 + 1, n_0 + 2, \ldots$, such that $\overline{\omega}(t_n) = n\pi + \vartheta_i + \bar{\vartheta}$. At each time instant t_n, according to the magnitude of $|\omega_i(t_n)|$, the following three cases should be discussed.

Case 1: When $|\omega_i(t_n)| = n\pi + \vartheta_i + \bar{\vartheta}$ for $i \in \{1, \ldots, 4\}$. By Lemma 2, we have $\Theta_i(|\omega_i(t_n)|) \leq -2^{-3}$, which together with (59) implies that

$$
\begin{aligned}
\Xi_i(t_n) \leq & -2^{-3} \underline{g}_i |\omega_i(t_n)| \exp\left(\omega_i^2(t_n)\right) \\
= & -2^{-3} \underline{g}_i (n\pi + \vartheta_i + \bar{\vartheta}) \exp\left((n\pi + \vartheta_i + \bar{\vartheta})^2\right) \quad (61)
\end{aligned}
$$

for all $|\omega_i(t_n)| = n\pi + \vartheta_i + \bar{\vartheta}$.

Case 2: When $n\pi + \vartheta_i \leq |\omega_i(t_n)| < n\pi + \vartheta_i + \bar{\vartheta}$ for $i \in \{1, \ldots, 4\}$. It follows from Lemma 2 that $\Theta_i(|\omega_i(t_n)|) \leq 0$. Thus, $\Xi_i(t_n) \leq 0$ for all $n\pi + \vartheta_i \leq |\omega_i(t_n)| < n\pi + \vartheta_i + \bar{\bar{\vartheta}}$.

Case 3: When $|\omega_i(t_n)| < n\pi + \vartheta_i$ for $i \in \{1, \ldots, 4\}$. Noting that $|\Theta_i(|\omega_i(t_n)|)| \leq 1$, we have

$$
\begin{aligned}
\Xi_i(t_n) \leq & \bar{g}_i |\omega_i(t_n)| \exp\left(\omega_i^2(t_n)\right) \\
= & \bar{g}_i (n\pi + \vartheta_i) \exp\left((n\pi + \vartheta_i)^2\right) \quad (62)
\end{aligned}
$$

for all $|\omega_i(t_n)| < n\pi + \vartheta_i$.

Noting that the number of elements in Case 1 is not less than 1, and the number of elements in Case 3 is not more than 3, one can arrive at

$$
\begin{aligned}
& \sum_{i=1}^{4} \Xi_i(t_n) + \sum_{i=1}^{4} |\omega_i(t_n)| \\
& \leq (n\pi + \vartheta_i + \bar{\vartheta}) \exp\left((n\pi + \vartheta_i)^2\right) \\
& \times \left[\begin{array}{l} -2^{-3}\underline{g}_i \exp(\bar{\vartheta}(\bar{\vartheta} + 2n\pi + 2\vartheta_i)) \\ +3\bar{g}_i + 4\exp(-(n\pi + \vartheta_i)^2) \end{array}\right] \quad (63)
\end{aligned}
$$

where $4\exp(-(n\pi + \vartheta_i)^2)$ decays to zero exponentially and $-2^{-3}\underline{g}_i \exp(\bar{\vartheta}(\bar{\vartheta} + 2n\pi + 2\vartheta_i)) \to -\infty$ as $n \to +\infty$. It is deduced from (63) that $\sum_{i=1}^{4} \Xi_i(t_n) + \sum_{i=1}^{4} |\omega_i(t_n)| \to -\infty$ as $n \to +\infty$, which apparently contradicts with (59). As a consequence, $\overline{\omega}(t)$ must be bounded, which in combination with (60) implies that $\omega_1(t)$, $\omega_2(t)$, $\omega_3(t)$, and $\omega_4(t)$ are bounded.

With the boundedness of $\omega_1(t)$, $\omega_2(t)$, $\omega_3(t)$, and $\omega_4(t)$, it can be seen from (59) that $\mathcal{L}$, $\widetilde{V}$, $\widetilde{h}$, $\widetilde{\gamma}$, $\widetilde{\alpha}$, and $\widetilde{Q}$ are bounded. Then, following similar analysis to [43], it can be concluded that all signals of the closed-loop system remain bounded. From (59), it holds that $\widetilde{x} \in L_2$ and $\widetilde{x} \in L_\infty$, $x \in \Omega_x$. Consequently, it follows from Barbalat's lemma that $\lim_{t \to +\infty} \widetilde{x} = 0$, $x \in \Omega_x$, which implies that the tracking errors $\widetilde{V}$ and $\widetilde{h}$ converge to zero asymptotically [53]–[56]. In addition, the boundedness of $\mathcal{L}$ leads to the boundedness of $\mathcal{L}_s$, which progressively implies that the full-state constraints are never violated. This completes the proof. ∎

Remark 3: It is worth mentioning that (59) encompasses 4 Nussbaum integral terms $\sum_{i=1}^{4} \int_0^{\omega_i} s_i g_i \mathcal{N}_i(\tau) d\tau$ where the signs of s_i might be distinct with each other [30]. This is because [29] and [30] have shown that it is still unclear how to establish boundedness $\sum_{i=1}^{4} \int_0^{\omega_i} s_i g_i \mathcal{N}_i(\tau) d\tau$ using conventional Nussbaum functions. Namely, if we adopt conventional Nussbaum functions, such as $\omega_i \sin(\omega_i^2)$ and $\cos(\omega_i) \exp(\omega_i)$, it would be possible that ω_i and ω_j ($i \neq j$) both approach infinity, while $\int_0^{\omega_i} s_i g_i \mathcal{N}_i(\tau) d\tau$ and $\int_0^{\omega_j} s_j g_j \mathcal{N}_j(\tau) d\tau$ counteract each other through taking opposite signs such that the summation term $\sum_{i=1}^{4} \int_0^{\omega_i} s_i g_i \mathcal{N}_i(\tau) d\tau$ still make (59) hold true. On the contrary, we develop a novel Nussbaum function as in (15) whose sign keeps the same on some periods of time even if each Nussbaum function has a different frequency, which successfully avoids the cancellation of different Nussbaum integral terms as shown in the proof after (60).

Remark 4: According to configuration designed in (15) and (16), it is concluded that $\int_0^{\omega_i} \mathcal{N}_i(\tau) d\tau$ is an even function of ω_i, thus we can calculate $\int_0^{\omega_i} \mathcal{N}_i(\tau) d\tau$ as $\int_0^{|\omega_i|} \mathcal{N}_i(\tau) d\tau$
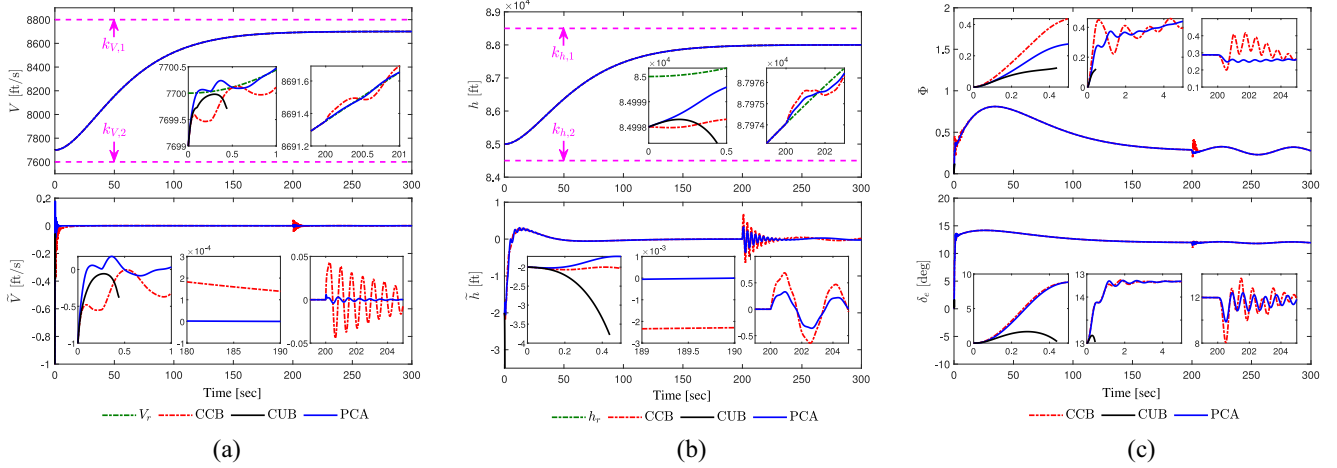
Fig. 4. Tracking performances and control inputs under three control schemes. (a) Tracking performances of velocity. (b) Tracking performances of altitude. (c) Control inputs.

without any concern on the sign of ω_i. In view of (63), $\int_0^{\omega_i} s_i g_i \mathcal{N}_i(\tau)d\tau$ and $\int_0^{\omega_j} s_j g_j \mathcal{N}_j(\tau)d\tau$ take the same sign and reinforce rather than counteract each other as long as $|\omega_i|$ and $|\omega_j|$ $(i \neq j)$ enter the same interval, which paves the way to find a contradiction of (59) that $\lim_{n \to +\infty} N(t_n) = -\infty$ once $\overline{\omega}$ is unbounded. Consequently, the Nussbaum functions (15) can handle the difficulty stemming from the multiple unknown control directions.

Remark 5: Despite the state-of-the-art design in [57] studied the same problem as our work, it has been shown in [58] that Lemma 1 of [57] only can guarantee the boundedness on finite-time interval $[0, t_f)$ with $t_f < \infty$. When $t_f = \infty$, the boundedness is lost due to ineffective handling of the terms, such as unmatched external disturbances and unknown time-varying nonlinearities. To overcome this difficulty, we designed an integrable function $\sigma(t)$ in control laws to robustly tackle the disturbances novelly, such that t_f could be extended to infinity.

V. SIMULATION RESULTS

In order to illustrate the effectiveness and superiority of the proposed constrained asymptotic tracking control scheme (PCA) for HFVs, several simulations are conducted in this section. The vehicle climbs a maneuver from initial values $h = 88\,000$ ft and $V = 7700$ ft/s to final values $h = 91\,000$ ft and $V = 8700$ ft/s. The reference commands of V_{ref} and h_{ref} are generated using the second-order filters with bandwidth 0.03 rad/s and damping 0.95. Based on practical engineering characteristics, the limitations of the actuators are set as $\Phi \in [0.05, 1.2]$ and $\delta_e \in [-20 \text{ deg}, 20 \text{ deg}]$.

In simulation, the HFVs model parameters are borrowed from [1], and the full-state constraints are selected as $k_{V,1} = 8800$ ft/s, $k_{V,2} = 7600$ ft/s, $k_{h,1} = 88\,500$ ft, $k_{h,2} = 84\,500$ ft, $k_{\gamma,1} = 0.3$ deg, $k_{\gamma,2} = 0.05$ deg, $k_{\alpha,1} = 2.2$ deg, $k_{\alpha,2} = -1$ deg, $k_{Q,1} = 2$ deg/s, and $k_{Q,2} = 1.5$ deg/s. The control parameters are chosen as $\kappa_V = 2.5$, $l_V = 3$, $\kappa_h = 1.5$, $l_h = 2$, $\kappa_\gamma = l_\gamma = 2$, $\kappa_\alpha = l_\alpha = 2$, $\kappa_Q = 50$, $l_Q = 2$, and $\sigma = 1/(0.1 + t^2)$. Parameters for adaptive laws are set

as $\Gamma_x = 5I$, $\rho_x = \upsilon_z = 0.5$, $x \in \Omega_x$, $z \in \Omega_z$. The positive filter parameters are selected as $\tau_z = 0.5$, $z \in \Omega_z$. The initial state variables are set as $V = 7699$ ft/s, $h = 87999$ ft, $\gamma = 0$ deg, $\alpha = 1.6325$ deg, and $Q = 0$ deg/s, and the initial values of $\widehat{W}_x$, $\widehat{\Psi}_x$, $\widehat{\Upsilon}_z$, $x \in \Omega_x$, $z \in \Omega_z$ are selected as zero. Besides, the uncertain aerodynamic coefficients are modeled as $C_i = C_i^*(1 + \Delta_i)$, where C_i^* represents the nominal coefficient and Δ_i represents the uncertain factor ranging from -20% to 20%. The external disturbances $\sin([\pi/30]t)$, $2\sin([\pi/30]t)$ are added to the velocity and altitude dynamics, respectively, when $t > 200$ s.

A. Comparative Simulations Under Three Control Schemes

In this section, to validate the superiority of PCA in achieving zero-error tracking and in tackling unknown control directions, PCA is compared with the conventional bounded tracking control (CCB) considering unknown control directions [43] and the bounded tracking control (CUB) without considering unknown control directions [17]. Simulation results can be seen in Figs. 4–6. Fig. 4(a) and (b) reveal that our proposed control scheme provides a better transient and steady state performance than that of [17] and [43], and guarantees the tracking errors $\widetilde{V}$ and $\widetilde{h}$ eventually converge to zero rather than the bounded ones as achieved by CCB and CUB. Fig. 4(c) shows the control inputs Φ and δ_e of PCA and CCB remain bounded, whereas the control signal of CUB diverges in the early stage due to the ineffective handling of unknown control directions. The zooms in Fig. 5(a)–(e) indicate that the proposed control method exhibits smoother response of γ, α, Q, η_1, and η_2 over CCB and that the various state variables of CUB diverge due to the presence of unknown control directions. Fig. 5(f)–(j) suggests that the trajectories of $\widehat{W}_x$, $\widehat{\Psi}_x$, $\widehat{\Upsilon}_z$, $x \in \Omega_x$, and $z \in \Omega_z$ remain bounded. Furthermore, integral absolute error (IAE) [$\int_0^T |e(t)|dt$], integral time absolute error (ITAE) [$\int_0^T t|e(t)|dt$], and root mean square error (RMSE) $[(1/T) \int_0^T e^2(t)dt]^{(1/2)}$ are utilized here as performance indices to evaluate the tracking performances of PCA, CUB, and CCB quantitatively. In addition, the control indexes are defined as
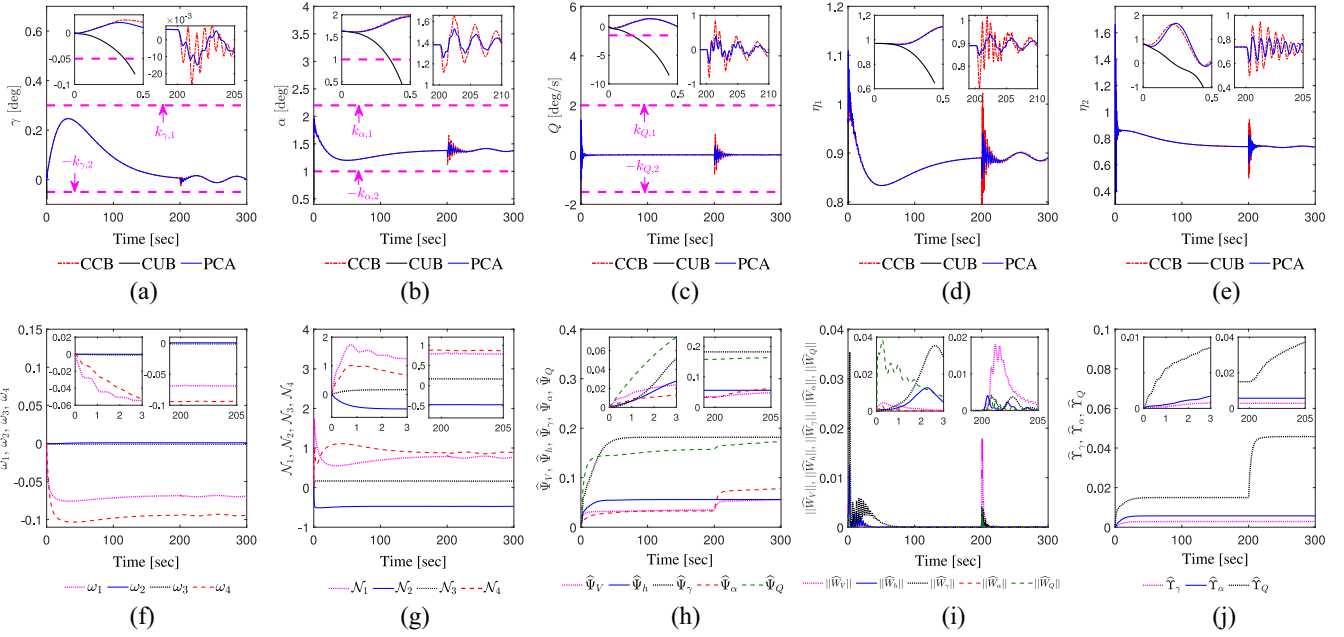
Fig. 5. Attitude angles, flexible states, and weight values under three control schemes. (a) Flight path angle γ. (b) Angle of attack α. (c) Pitch rate Q. (d) Flexible state η_1. (e) Flexible state η_2. (f) Responses of ω_i. (g) Responses of $\mathcal{N}_i$. (h) Responses of $\widehat{\Psi}_x$. (i) Responses of $\|\widehat{W}_x\|$. (j) Responses of $\widehat{\Upsilon}_z$.

TABLE I
PERFORMANCE INDICES UNDER THREE CONTROL SCHEMES

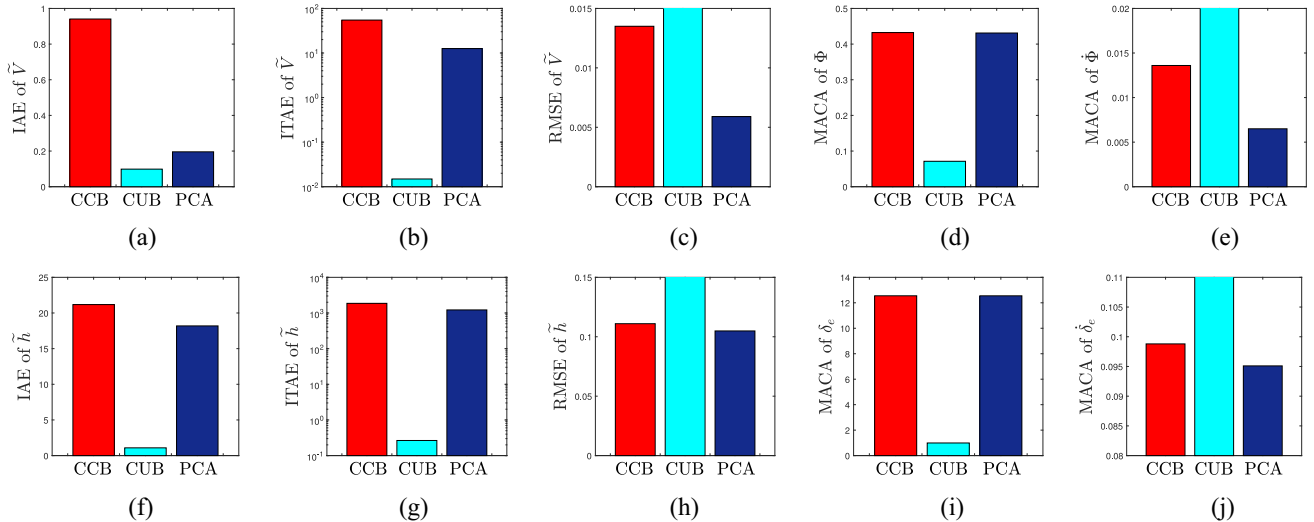| Control Method	Velocity Channel			Altitude Channel			Fuel Equivalence Ratio		Deflection of Elevator	
	IAE	ITAE	RMSE	IAE	ITAE	RMSE	Φ	$\dot{\Phi}$	δ_e	$\dot{\delta}_e$
CCB	0.9407	54.8299	0.0135	21.1771	1864.4	0.1110	0.4323	0.0136	12.5516	0.0998
CUB	0.0986	0.0149	0.2265	1.0880	0.2654	1.7929	0.0713	4.4589	0.9914	64.8442
PCA	0.1958	12.5634	0.0059	18.1901	1220	0.1049	0.4311	0.0065	12.5501	0.0951

Fig. 6. Various performance indices under three control schemes. (a) IAE of $\tilde{V}$. (b) ITAE of $\tilde{V}$. (c) RMSE of $\tilde{V}$. (d) MACA of Φ. (e) MACA of Φ. (f) IAE of $\tilde{h}$. (g) ITAE of $\tilde{h}$. (h) RMSE of $\tilde{h}$. (i) MACA of δ_e. (j) MACA of δ_e.

the mean absolute control actions (MACA) $[(1/T)\int_0^T |\Phi|dt]$, $[(1/T)\int_0^T |\dot{\Phi}|dt]$, $[(1/T)\int_0^T |\delta_e|dt]$, and $[(1/T)\int_0^T |\dot{\delta}_e|dt]$. The calculation results are summarized in Table I and Fig. 6 shows that our developed method requires less control efforts than that of CCB and CUB, which validates the effectiveness of

the proposed control method. To investigate the impact of different initial values on our proposed Nussbaum functions (15), some further simulations are conducted in this scenario by taking the following two cases into consideration. The simulation result is provided in Fig. 7.
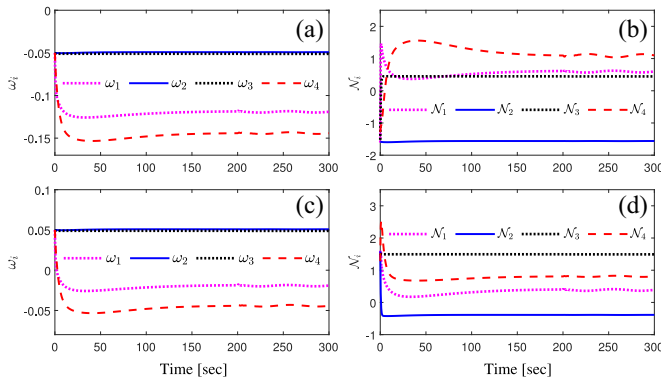
Fig. 7. (a) ω_i in Case 1. (b) $\mathcal{N}_i$ in Case 1. (c) ω_i in Case 2. (d) $\mathcal{N}_i$ in Case 2.

1) *Case 1:* $\omega_i(0) = -0.05$, $i = 1, \ldots, 4$.
2) *Case 2:* $\omega_i(0) = 0.05$, $i = 1, \ldots, 4$.

It can concluded from Fig. 7 that our newly proposed Nussbaum functions can still preserve the boundedness of adaptation parameters ω_i and Nussbaum functions $\mathcal{N}_i$, $i = 1, \ldots, 4$ under two different sets of initial conditions.

VI. CONCLUSION

This article presents a result about zero-errors accurate tracking control for the longitudinal dynamics of HFVs in the presence of multiple unknown control directions and asymmetric flight state constraints. The distinguishing characteristic of our design arises in proposing a class of new Nussbaum function, which not only guarantees the boundedness of the summation of multiple Nussbaum integral terms but the boundedness of each individual Nussbaum integral term. By means of Barbalat's lemma, the velocity and altitude tracking errors can been shown to converge to zero rather than a residual set. Asymmetric integral Lyapunov functions are utilized to ensure that flight state variables are kept within some compact sets all the time. Future research will be focused on the consensus tracking problem of HFV swarm systems [59]–[62] and the trajectories tracking problem of HFVs with switched dynamics [63]–[71].

REFERENCES

[1] J. T. Parker, A. Serrani, S. Yurkovich, M. A. Bolender, and D. B. Doman, "Control-oriented modeling of an air-breathing hypersonic vehicle," *J. Guid. Control Dyn.*, vol. 30, no. 3, pp. 856–869, 2007.

[2] X. X. Hu, B. Xu, and C. H. Hu, "Robust adaptive fuzzy control for HFV with parameter uncertainty and unmodeled dynamics," *IEEE Trans. Ind. Electron.*, vol. 65, no. 11, pp. 8851–8860, Nov. 2018.

[3] M. Lv, Y. Li, W. Pan, and S. Baldi, "Finite-time fuzzy adaptive constrained tracking control for hypersonic flight vehicles with singularity-free switching," *IEEE/ASME Trans. Mechatronics*, early access, Jun. 18, 2021, doi: 10.1109/TMECH.2021.3090509.

[4] Q. Shen, B. Jiang, and V. Cocquempot, "Fuzzy logic system-based adaptive fault-tolerant control for near-space vehicle attitude dynamics with actuator faults," *IEEE Trans. Fuzzy Syst.*, vol. 21, no. 2, pp. 289–300, Apr. 2013.

[5] R. Zuo, Y. Li, M. Lv, Z. Liu, and Z. Dong, "Design of singularity-free fixed-time fault-tolerant control for HFVs with guaranteed asymmetric time-varying flight state constraints," *Aerosp. Sci. Technol.*, vol. 120, Jan. 2022, Art. No. 107270.

[6] B. Xu, Y. Shou, J. Luo, H. Pu, and Z. Shi, "Neural learning control of strict-feedback systems using disturbance observer," *IEEE Trans. Neural Netw. Learn. Syst.*, vol. 30, no. 5, pp. 1269–1307, May 2019.

[7] L. Fiorentini and A. Serrani, "Adaptive restricted trajectory tracking for a non-minimum phase hypersonic vehicle model," *Automatica*, vol. 48, no. 7, pp. 1248–1261, 2012.

[8] Q. Shen, B. Jiang, and V. Cocquempot, "Fault tolerant control for T-S fuzzy systems with application to near-space hypersonic vehicle with actuator faults," *IEEE Trans. Fuzzy Syst.*, vol. 20, no. 4, pp. 652–665, Aug. 2012.

[9] M. A. Bolender and D. B. Doman, "Nonlinear longitudinal dynamical model of an air-breathing hypersonic vehicle," *J. Spacecr. Rockets*, vol. 44, no. 2, pp. 374–387, Mar. 2007.

[10] L. Fiorentini, A. Serrani, M. A. Bolender, and D. B. Doman, "Nonlinear robust adaptive control of flexible air-breathing hypersonic vehicles," *J. Guid. Control Dyn.*, vol. 32, no. 2, pp. 401–416, Mar. 2009.

[11] R. Zuo, Y. Li, M. Lv, X. Wang, and Z. Liu, "Realization of trajectory precise tracking for hypersonic flight vehicles with prescribed performances," *Aerosp. Sci. Technol.*, vol. 111, Apr. 2021, Art. no. 106554.

[12] Z. Liu, X. Tan, R. Yuan, G. Fan, and J. Yi, "Immersion and invariancebased output feedback control of air-breathing hypersonic vehicles," *IEEE Trans. Autom. Sci. Eng.*, vol. 13, no. 1, pp. 394–402, Jan. 2016.

[13] J. Sun, Z. Pu, J. Yi, and Z. Liu, "Fixed-time control with uncertainty and measurement noise suppression for hypersonic vehicles via augmented sliding mode observers," *IEEE Trans. Ind. Informat.*, vol. 16, no. 2, pp. 1192–1203, Feb. 2020.

[14] H. Xu, M. Mirmirani, and P. Ioannou, "Adaptive sliding mode control design for a hypersonic flight vehicle," *J. Guid. Control Dyn.*, vol. 27, pp. 829–838, Sep. 2004.

[15] Q. Zong, J. Wang, B. Tian, and Y. Tao, "Quasi-continuous high-order sliding mode controller and observer design for flexible hypersonic vehicle," *Aerosp. Sci. Technol.*, vol. 27, pp. 127–137, Jun. 2013.

[16] J. Sun, J. Yi, Z. Pu, and Z. Liu, "Adaptive fuzzy nonsmooth backstepping output-feedback control for hypersonic vehicles with finite-time convergence," *IEEE Trans. Fuzzy Syst.*, vol. 28, no. 10, pp. 2320–2334, Oct. 2020, doi: 10.1109/TFUZZ.2019.2934934.

[17] X. Bu, "Air-breathing hypersonic vehicles funnel control using neural approximation of non-affine dynamics," *IEEE/ASME Trans. Mechatronics*, vol. 23, no. 5, pp. 2099–2108, Oct. 2018.

[18] X. Bu, "Envelope-constraint-based tracking control of air-breathing hypersonic vehicles," *Aerosp. Sci. Technol.*, vol. 95, Dec. 2019, Art. no. 105429.

[19] Z. Zhang, Y. Song, and C. Wen, "Adaptive decentralized output-feedback control dealing with static/dynamic interactions and different-unknown subsystem control directions," *IEEE Trans. Autom. Control*, vol. 66, no. 8, pp. 3818–3824, Aug. 2021, doi: 10.1109/TAC.2020.3028563.

[20] J. Shaughnessy, S. Pickney, and J. McMinn, "Hypersonic vehicle simulation model: Winged-cone configuration," NASA Langley Res. Center, Hampton, VA, USA, Rep. TM-102610, 1990.

[21] B. Xu, R. Qi, and B. Jiang, "Adaptive fault-tolerant control for HSV with unknown control direction," *IEEE Trans. Aerosp. Electron. Syst.*, vol. 55, no. 6, pp. 2743–2758, Dec. 2019.

[22] R. D. Nussbaum, "Some remarks on the conjecture in parameter adaptive control," *Syst. Control Lett.*, vol. 3, no. 5, pp. 243–246, Nov. 1983.

[23] X. Ye, "Asymptotic regulation of time-varying uncertain nonlinear systems with unknown control directions," *Automatica*, vol. 35, pp. 929–935, May 1999.

[24] S. S. Ge and J. Wang, "Robust adaptive neural control for a class of perturbed strict feedback nonlinear systems," *IEEE Trans. Neural Netw. Learn. Syst.*, vol. 13, no. 6, pp. 1409–1419, Nov. 2002.

[25] Y. Liu and S. Tong, "Barrier Lyapunov functions for Nussbaum gain adaptive control of full state constrained nonlinear systems," *Automatica*, vol. 76, pp. 143–152, Feb. 2017.

[26] S. S. Ge and J. Wang, "Robust adaptive tracking for time-varying uncertain nonlinear systems with unknown control coefficients," *IEEE Trans. Autom. Control*, vol. 48, no. 8, pp. 1463–1469, Aug. 2003.

[27] M. Lv, W. Yu, J. Cao, and S. Baldi, "Consensus in high-power multi-agent systems with mixed unknown control directions via hybrid Nussbaum-based control," *IEEE Trans. Cybern.*, early access, Nov. 4, 2020, doi: 10.1109/TCYB.2020.3028171.

[28] Z. Chen, "Nussbaum functions in adaptive control with time-varying unknown control coefficients," *Automatica*, vol. 102, pp. 72–79, Apr. 2019.

[29] X. Ye and J. Jiang, "Adaptive nonlinear design without a priori knowledge of control directions," *IEEE Trans. Autom. Control*, vol. 43, no. 11, pp. 1617–1621, Nov. 1998.

[30] J. Huang, W. Wang, C. Wen, and J. Zhou, "Adaptive control of a class of strict-feedback time-varying nonlinear systems with unknown control coefficients," *Automatica*, vol. 93, pp. 98–105, Jul. 2018.

[31] W. Chen, X. Li, W. Ren, and C. Wen, "Adaptive consensus of multi-agent systems with unknown identical control directions based on a novel Nussbaum-type function," *IEEE Trans. Autom. Control*, vol. 59, no. 7, pp. 1887–1892, Jul. 2014.

[32] C. Chen, C. Wen, Z. Liu, K. Xie, Y. Zhang, and C. L. P. Chen, "Adaptive consensus of nonlinear multi-agent systems with non-identical partially unknown control directions and bounded modelling errors," *IEEE Trans. Autom. Control*, vol. 62, no. 9, pp. 4654–4659, Sep. 2017.

[33] K. Zhao and Y. Song, "Removing the feasibility conditions imposed on tracking control designs for state-constrained strict-feedback systems," *IEEE Trans. Autom. Control*, vol. 64, no. 3, pp. 1265–1272, Mar. 2019.

[34] L. Tang, D. Ma, and J. Zhao, "Adaptive neural control for switched nonlinear systems with multiple tracking error constraints," *IET Signal Process.*, vol. 13, no. 3, pp. 330–337, 2019, doi: 10.1049/iet-spr.2018.5077.

[35] K. Zhao, Y. Song, and Z. Zhang, "Tracking control of MIMO nonlinear systems under full state constraints: A single parameter adaptation approach free from feasibility conditions," *Automatica*, vol. 55, no. 8, pp. 52–60, 2019.

[36] K. P. Tee and S. S. Ge, "Barrier Lyapunov functions for the control of output-constrained nonlinear systems," *Automatica*, vol. 45, pp. 918–927, Apr. 2009.

[37] B. Xu, Z. Shi, F. Sun, and W. He, "Barrier Lyapunov function based learning control of hypersonic flight vehicle with AOA constraint and actuator faults," *IEEE Trans. Cybern.*, vol. 49, no. 3, pp. 1047–1057, Mar. 2019.

[38] K. Zhao, Y. Song, C. L. P. Chen, and L. Chen, "Control of nonlinear systems under dynamic constraints: A unified barrier function based approach," *Automatica*, vol. 56, no. 9, pp. 1–9, 2020.

[39] S. S. Ge, C. Hang, and T. Zhang, "A direct adaptive controller for dynamic systems with a class of nonlinear parameterizations," *Automatica*, vol. 35, pp. 741–747, Apr. 1999.

[40] K. P. Tee and S. S. Ge, "Control of state-constrained nonlinear systems using integral barrier Lyapunov functionals," in *Proc. 51st IEEE Conf. Decis. Control*, Dec. 2012, pp. 3239–3244.

[41] L. Liu, T. Gao, Y. Liu, S. Tong, C. L. P. Chen, and L. Ma, "Time-varying IBLFs-based adaptive control of uncertain nonlinear systems with full state constraints," *Automatica*, vol. 129, Jul. 2021, Art. no. 109595.

[42] B. Liu, M. Hou, J. Ni, Y. Li, and Z. Wu, "Asymmetric integral barrier Lyapunov function-based adaptive tracking control considering full-state with input magnitude and rate constraint," *J. Franklin Inst.*, vol. 357, pp. 9709–9732, Sep. 2020.

[43] C. Wang, C. Wen, and L. Guo, "Multivariable adaptive control with unknown signs of the high-frequency gain matrix using novel Nussbaum functions," *Automatica*, vol. 111, Jan. 2020, Art. no. 108618.

[44] L. Wang, *Adaptive Fuzzy Systems and Control: Design and Stability Analysis*. Englewood Cliffs, NJ, USA: Prentice Hall, 1994.

[45] J. Dong, Y. Wu, and G. Yang, "A new sensor fault isolation method for T-S fuzzy systems," *IEEE Trans. Cybern.*, vol. 47, no. 9, pp. 2437–2447, Sep. 2017.

[46] Z. Zhang, H. Liang, C. Wu, and C. K. Ahn, "Adaptive event-triggered output feedback fuzzy control for nonlinear networked systems with packet dropouts and actuator failure," *IEEE Trans. Fuzzy Syst.*, vol. 27, no. 9, pp. 1793–1806, Sep. 2019.

[47] D. Li, L. Liu, Y. Liu, S. Tong, and C. L. P. Chen, "Fuzzy approximation-based adaptive control of nonlinear uncertain state constrained systems with time-varying delays," *IEEE Trans. Fuzzy Syst.*, vol. 28, no. 8, pp. 1620–1630, Aug. 2020.

[48] X. Zhao and H. Yang, "Adaptive fuzzy hierarchical sliding mode control for a class of MIMO nonlinear time-delay systems with input saturation," *IEEE Trans. Fuzzy Syst.*, vol. 25, no. 5, pp. 1062–1077, Oct. 2017.

[49] H. Liang, X. Guo, Y. Pan, and T. Huang, "Event-triggered fuzzy bipartite tracking control for network systems based on distributed reduced-order observers," *IEEE Trans. Fuzzy Syst.*, vol. 29, no. 6, pp. 1601–1614, Jun. 2021, doi: 10.1109/TFUZZ.2020.2982618.

[50] M. Lv, W. Yu, and S. Baldi, "The set-invariance paradigm in fuzzy adaptive DSC design of large-scale nonlinear input-constrained systems," *IEEE Trans. Syst., Man, Cybern., Syst.*, vol. 51, no. 2, pp. 1035–1045, Feb. 2021.

[51] D. Swaroop, J. K. Hedrick, P. P. Yip, and J. C. Gerdes, "Dynamic surface control for a class of nonlinear systems," *IEEE Trans. Autom. Control*, vol. 45, no. 10, pp. 1893–1899, Oct. 2000.

[52] H. Deng and M. Krstic, "Stochastic nonlinear stabilization—I: A backstepping design," *Syst. Control Lett.*, vol. 32, pp. 143–150, Nov. 1997.

[53] Y. Li and S. Tong, "A bound estimation approach for adaptive fuzzy asymptotic tracking of uncertain stochastic nonlinear systems," *IEEE Trans. Cybern.*, early access, Nov. 10, 2020, doi: 10.1109/TCYB.2020.3030276.

[54] T. Lei, W. Meng, K. Zhao, and L. Chen, "Adaptive asymptotic tracking control of constrained MIMO nonlinear systems via event-triggered strategy," *Int. J. Robust Nonlinear Control*, vol. 31, no. 5, pp. 1479–1496, 2020, doi: 10.1002/rnc.5372.

[55] X. Zhao, X. Wang, L. Ma, and G. Zong, "Fuzzy-approximation-based asymptotic tracking control for a class of uncertain switched nonlinear systems," *IEEE Trans. Fuzzy Syst.*, vol. 28, no. 4, pp. 632–644, Apr. 2020.

[56] Y. Li, X. Hu, W. Che, and Z. Hou, "Event-based adaptive fuzzy asymptotic tracking control of uncertain nonlinear systems," *IEEE Trans. Fuzzy Syst.*, vol. 29, no. 10, pp. 3003–3013, Oct. 2021, doi: 10.1109/TFUZZ.2020.3010643.

[57] H. Ye and B. Jiang, "Adaptive switching control for hypersonic vehicle with uncertain control direction," *J. Franklin Inst.*, vol. 357, no. 13, pp. 8851–8869, 2020, doi: 10.1016/j.jfranklin.2020.06.014.

[58] H. E. Psillakis, "Further results on the use of nussbaum gains in adaptive neural network control," *IEEE Trans. Autom. Control*, vol. 55, no. 12, pp. 2841–2846, Dec. 2010.

[59] P. Shi and Q. K. Shen, "Cooperative control of multi-agent systems with unknown state-dependent controlling effects," *IEEE Trans. Autom. Sci. Eng.*, vol. 12, no. 3, pp. 827–834, Jul. 2015.

[60] G. Zong, H. Ren, and H. R. Karimi, "Event-triggered communication and annular finite-time H_∞ filtering for networked switched systems," *IEEE Trans. Cybern.*, vol. 51, no. 1, pp. 309–317, Jan. 2021.

[61] H. Ren, G. Zong, and T. Li, "Event-triggered finite-time control for networked switched linear systems with asynchronous switching," *IEEE Trans. Syst., Man, Cybern., Syst.*, vol. 48, no. 11, pp. 1874–1884, Nov. 2018.

[62] H. Liang, Y. Zhang, T. Huang, and H. Ma, "Prescribed performance cooperative control for multiagent systems with input quantization," *IEEE Trans. Cybern.*, vol. 50, no. 5, pp. 1810–1819, May 2020.

[63] L. Ma, N. Xu, X. Zhao, G. Zong, and X. Huo, "Small-gain technique based adaptive neural output-feedback fault-tolerant control of switched nonlinear systems with unmodeled dynamics," *IEEE Trans. Syst., Man, Cybern., Syst.*, vol. 51, no. 11, pp. 7051–7062, Nov. 2021, doi: 10.1109/TSMC.2020.2964822.

[64] D. Yang, G. Zong, and H. R. Karimi, "H_∞ refined antidisturbance control of switched LPV systems with application to aero-engine," *IEEE Trans. Ind. Electron.*, vol. 67, no. 4, pp. 3180–3190, Apr. 2020.

[65] S. Sui, C. L. P. Chen, and S. Tong, "Neural network filtering control design for nontriangular structure switched nonlinear systems in finite time," *IEEE Trans. Neural Netw. Learn. Syst.*, vol. 30, no. 7, pp. 2153–2162, Jul. 2019.

[66] S. Sui, C. L. P. Chen, and S. Tong, "A novel adaptive NN prescribed performance control for stochastic nonlinear systems," *IEEE Trans. Neural Netw. Learn. Syst.*, vol. 32, no. 7, pp. 3196–3205, Jul. 2021, doi: 10.1109/TNNLS.2020.3010333.

[67] K. Zhao, Y. Song, and L. Chen, "Tracking control of nonlinear systems with improved performance via transformational approach," *Int. J. Robust Nonlinear Control*, vol. 29, no. 6, pp. 1789–1806, 2019.

[68] M. Lv, B. De Schutter, C. Shi, and S. Baldi, "Logic-based distributed switching control for agents in power chained form with multiple unknown control directions," *Automatica*, vol. 137, Jan. 2022, Art. no. 110143.

[69] G. Zong, H. Sun, and S. K. Nguang, "Decentralized adaptive neuro-output feedback saturated control for INS and its application to AUV," *IEEE Trans. Neural Netw. Learn. Syst.*, vol. 32, no. 12, pp. 5492–5501, Dec. 2021, doi: 10.1109/TNNLS.2021.3050992.

[70] M. Lv, W. Yu, J. Cao, and S. Baldi, "A separation-based methodology to consensus tracking of switched high-order nonlinear multi-agent systems," *IEEE Trans. Neural Netw. Learn. Syst.*, early access, Apr. 14, 2021, doi: 10.1109/TNNLS.2021.3070824.

[71] M. Lv, B. De Schutter, W. Yu, and S. Baldi, "Adaptive asymptotic tracking for a class of uncertain switched positive compartmental models with application to anesthesia," *IEEE Trans. Syst., Man, Cybern., Syst.*, vol. 51, no. 8, pp. 4936–4942, Aug. 2021, doi: 10.1109/TSMC.2019.2945590.